AN ABSTRACT OF THE THESIS OF

Rachel R. Holser for the degree of Master of Science in Oceanography on March 11, 2010.

Title: High-Resolution Sampling of Particulate Organic Carbon in a Coastal Upwelling System.

Abstract approved:

Miguel A. Goñi Burke Hales

Summertime, wind-driven upwelling off the Oregon coast delivers nutrient rich water to the surface that fuels the autotrophic production of particulate organic carbon (POC). This POC can be transported horizontally by fluid motions and vertically by sinking to the bottom where it can be entrained in the benthic boundary layer (BBL). POC can be transformed during transport by heterotrophic metabolism, thus changing its concentration and composition. To better understand the dynamics of POC within the water column of this highly variable system, we developed a semi-automated filtration system that, when coupled to a towed profiling/sampling vehicle, allowed us to collect POC samples at higher spatial and temporal resolution than previously possible. During late May of 2009 we used this system to collect around 400 POC samples from two cross-shelf transects off the central Oregon coast spanning the ranges between BBL and surface mixed layer, and shelfbreak to shoreline. These samples were collected in conjunction with in-situ measurements of temperature, salinity, chlorophyll fluorescence, optical backscatter, and beam attenuation coefficients. Analyses of both the optical and bulk measurements indicate the presence of three distinct particle pools. The first pool is rich in POC and shows

elevated fluorescence and beam-c relative to optical backscatter. The second pool is elevated in both fluorescence and optical backscatter, and is rich in POC relative to beam-c. The third pool is depleted in POC and shows proportionately elevated backscatter. Using variations in the optical properties of these three particle pools, we created multiple POC – beam-c calibrations, which allowed us to derive high-resolution POC distributions within the water column. This derived distribution indicates a decoupling between sediment and carbon in the BBL, and an unanticipated elevation of POC in the mid water column.

High-Resolution Sampling of Particulate Organic Carbon in a Coastal Upwelling System

by
Rachel R. Holser

A THESIS

Submitted to

Oregon State University

in partial fulfillment of
the requirements for the
degree of

Master of Science

Presented March 11, 2010
Commencement June 2010

Master of Science thesis of Rachel R. Holser presented on March 11, 2010.

APPROVED:

Co-Major Professor, representing Oceanography

Co-Major Professor, representing Oceanography

Dean of the College of Oceanic and Atmospheric Sciences

Dean of the Graduate School

I understand that my thesis will become part of the permanent collection of Oregon State University libraries. My signature below authorizes release of my thesis to any reader upon request.

Rachel R. Holser, Author

ACKNOWLEDGMENTS

First, I would like to thank my advisor, Dr. Miguel Goñi, for all of his help and support, both financially and academically. I would also like to thank Dr. Burke Hales for his help and unwavering honesty in pointing out where I screw up and how I can improve. Thank you to my other committee members, Dr. Zanna Chase and Dr. Kipp Shearman, for your input and advice during this process.

I cannot thank the students and techs I've worked with over the last few years enough. In particular, thank you to Beth, Sam, Chris, and Dave for all the time spent on Wecoma. Whether we were working, talking, laughing, or watching Big Bang Theory, I treasured all of your company, help, advice, and contributions to my quote book.

To my lab/office partner Roxanne: you are an incredible (and brilliant) woman, and your support and input have helped enormously over the last year and a half. Thank you for climbing with me, for enduring classes with me, and for being there to talk, whether it was about my project or anything else. And, I suppose, for teaching me how to belly dance. A little.

All of the work I have accomplished in the last several years would have been vastly more difficult without the dedicated help of our research assistant Yvan and a host of undergraduate students. Thank you all for your time and patience with folding samples…and more samples…and more samples…

My family has always been an amazing support, and certainly no less over the last few years. Thank you for listening to my complaints about how things are hard. And thank you for then calmly reminding me that hard isn't a bad thing, and I am in fact learning so many lessons about life. Thank you for helping me with odds and ends, whether it is building a box or proofreading a poster. Thank you so much for your patience.

To all of my non-oceanography friends, you have all in some way helped me along the road, whether it was just listening after I had a hard day, running or climbing with me, looking over my writing, or linking me a particularly pertinent (or just funny) xkcd. Kristina, Alicia, Becca, Eric, Jason, Eli, Kyle: you are all amazing friends.

Lastly, I'd like to thank Dave. Although you've been a more recent addition to the world of Rachel, I cannot express enough how much your support and encouragement has helped me over the last months. You are an incredibly talented and dedicated worker, and you have inspired me to push myself that much harder.

Thank you all.

TABLE OF CONTENTS

LIST OF FIGURES

LIST OF FIGURES (continued)

LIST OF FIGURES (continued)

LIST OF TABLES

LIST OF APPENDIX FIGURES

LIST OF APPENDIX FIGURES (continued)

LIST OF APPENDIX TABLES

1. Introduction

Upwelling systems are a small but vital part of coastal margins. In Oregon's coastal margin, wind-driven upwelling takes place throughout the summer as alongshore northerly winds cause divergence of water from the coastline. The resulting Ekman transport moves water from below 200m depth up into the bottom boundary layer (BBL) of the continental shelf. This cold, dense water mass often moves upward along the shelf as far as the euphotic zone (Lenz and Trowbridge, 1991; 1998; Perlin et al., 2005), and is rich with nutrients released from the respiratory degradation of organic matter. When these nutrients reach the surface, either through direct transport or through turbulent mixing (Hales et al., 2005), they are quickly utilized by phytoplankton communities.

While only 10% of the world's oceans are coastal margins, they account for up to 40% of ocean carbon sequestration (Muller-Karger et al., 2005). Upwelling systems comprise an even smaller segment of the ocean (1% of the global ocean and 10% of coastal margins), yet they account for up to 10% of global new production (Chavez and Toggweiler, 1995). New production is based on nitrate, nitrogen that is newly available for uptake, as opposed to regenerated ammonia (Dugdale and Goering, 1967). Consequently, new production represents an addition of organic carbon to the ocean reservoir. Recent incubation studies (Wetz and Wheeler, 2003) done on Oregon coastal waters show that a significant portion of the organic material resulting from new production is particulate rather than dissolved form. Given an appropriate export mechanism, this newly generated particulate organic carbon (POC) can be removed from the near-surface ocean and sequestered on longer time scales.

The advective dynamics of coastal upwelling systems are complex and may create transport pathways for the movement of particulate organic carbon (POC) off of the continental shelf and into the deep ocean potentially sequestering it on a multi-decadal scale, if not longer (Hales et al., 2006). Upwelling is not a continuous process; the intensity and rate of upwelling can vary significantly over the course of a season, and includes relaxation events when upwelling forcing eases or even reverses.

These events occur when the wind driving Ekman transport periodically dies down or reverses direction, reducing the divergence from the coastline that causes upwelling and resulting in a down-shelf slumping of the upwelling front (Barth and Wheeler, 2005). Relaxation events could provide a mechanism for particle export off the continental shelf. Coupled with the dominance of particulate new production, this implies that a significant portion of new production from the Oregon coastal margin could be sequestered in the deep ocean during the upwelling season.

In earlier studies, Hales et al. (2006) found high levels of new productivity based on O_2 budgets that were consistent with earlier productivity estimates (Dickson and Wheeler, 1995), and the observed draw-down of NO_3^- at that time (Hales et al., 2005). The POC produced during the summer months must either accumulate or be lost via respiration in the water column, or be exported from the system through burial or advective transport. Hales et al. (2006) found, however, that burial and respiration combined do not balance the amount of POC being produced during the upwelling season, yet there was a net sink of CO_2 into the coastal water. This discrepancy in the POC budget (as much as 10 tons of carbon per meter of coastline (Hales et al., 2006), could be explained by event-driven POC export during periods of relaxation.

Investigating POC export mechanisms requires a detailed understanding of the distribution and dynamics of particles within the system. Combining optical and physical measurements allows us to quantify and characterize the particle content of the water column. Optical measurements such as beam attenuation (c_p) and backscatter are established proxies for total particle content, and the ratio of backscatter to c_p relates to organic carbon content (Gardner et al., 2001; Boss et al., 2009). Chlorophyll fluorescence and beam attenuation have also been used to quantify and characterize phytoplankton biomass (Behrenfeld and Boss, 2003; 2006; Eisner and Cowles, 2005). Karp-Boss et al. (2004) used the relationship between c_p and particulate organic carbon to estimate high-resolution POC concentrations off the Oregon coast.

While optical properties are effective tools for understanding particle dynamics, they are limited by the quality and quantity of POC samples available for calibration. The manual filtration methods most commonly used for discrete POC sampling are slow and labor intensive. Sampling frequency is limited by the time required to homogenize, measure, and filter each sample by hand. Due to the limitations of historically used POC sampling methods, relatively few POC measurements have been available for comparison to optical properties.

Gardner et al. (2006) compiled samples of POC and c_p from a variety of times and locations around the globe. They examined 4456 data pairs from nine different locations spanning several years. The authors found that the relationship between the two properties showed significant spatial variability, with slopes ranging from 25.3 to 52.6, indicating that c_p is sensitive to the type of particle pool, as well as to carbon content. Sullivan et al. (2004) utilized optical properties, in conjunction with particle size distribution, to discriminate between three distinct particle types within the coastal ocean. These precedents suggest that combining improved POC sampling with composite optical measurements could improve our understanding of both the distribution and characteristics of POC.

To improve our understanding of particle dynamics within the Oregon coastal upwelling system, we developed a semi-automated filtration system intended for use in conjunction with a towed/pumping vehicle. Coupling *in situ* optical measurements with the resulting high-resolution chemical characterization of particles enables us to construct a more sensitive set of calibrations between optical properties and organic carbon content. This in turn allows us to extrapolate carbon distributions within the water column more precisely than is possible with either chemical analyses or optics alone, with the ultimate goal of detecting and quantifying POC export off of the continental shelf of the Oregon coast during an upwelling/relaxation cycle.

2. Methods

2.1. Instrument Design

2.1.1. Hardware

A semi-automated filtration systems (SAFS) was designed to collecting particulate samples from a pressurized sampling line. Briefly, a computer-controlled multi-position valve was interfaced with an electronic flow meter whose signal was continuously logged. Each outlet port of the valve was connected to a filter cartridge. At specified intervals, a different outlet port was selected, and when a specified amount of water was passed through that port and filter, the port was isolated. One port of the valve was reserved as a bypass line, allowing the system to be flushed

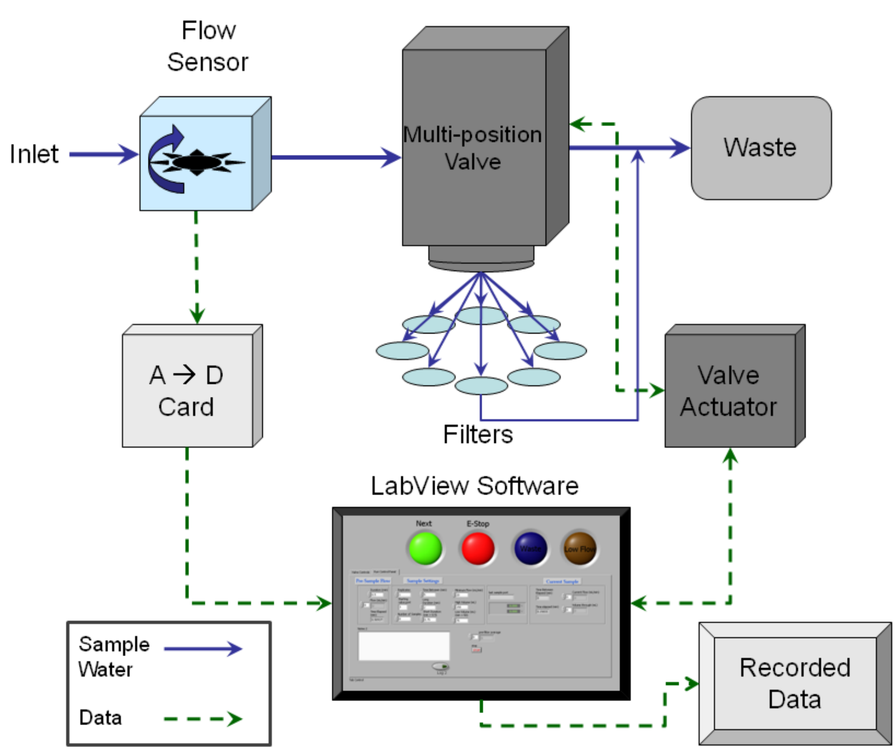

Figure 1 – Schematic depicting the flow of water (blue) and data (green) through the sampling system.

continuously when samples were not being collected.

Figure 1 depicts the SAFS, and its components are described below. PEEK tubing of 1/8 inch diameter was used to connect the system to the flowing seawater line. We used a MacMillan liquid flow meter, Flo-Sensor Model 101 (available at www.colepalmer.com, #EW-32703-50) to measure the flow rate coming off the seawater line. This rotameter-based flow sensor has a 13-100 mL/min range and a flow-proportional 0-5 volt analog DC output, which was captured and communicated to the system computer via the analog-digital conversion function of a National Instruments™ multifunction data acquisition card (available at www.ni.com, #NI USB-6009). We calibrated each flow sensor with timed, gravimetric flow tests to generate accurate flow-voltage relationships. A VICI® Cheminert® low pressure 10 position valve with a microelectric actuator, whose position was controlled by serial signals (available at www.vici.com, # C25-6180EMH), directed the sample flow to different filter holders connected to the valve ports. We used eight Swinney stainless 13mm filter holders containing Pall glass fiber filters (GF's) type A/E with a nominal pore diameter of 1.0 µm (both available from www.vwr.com, #28145-295 and #28150-134). All hardware components of the SAFS were mounted on a sheet of clear acrylic plastic, and this was installed near a sink or drain in the ship's laboratory.

2.1.2. Software

The system was controlled and operational data collected using a program we developed with LabView™ software. This program communicates with the valve actuator and records flow rate, flow volume and other sampling data via the data acquisition device described above. The basic functionality of the software is relatively simple: for most of the operational time, the valve was directed to sit in bypass mode, and water flowed through one designated port and to waste. At user-specified intervals, the flow was directed to a specified sample port and monitored for the duration of the filtration period. After either 1) a user-specified time had elapsed;

2) a total flow-volume had been achieved; or 3) the flow dropped below a specified minimum level, the valve was directed back to the bypass position until the next sample was to be collected. The total volume for each sample was calculated by integrating the flow rate over sampling time.

The number of samples that can be collected in a sequence is user-determined, but is limited by the number of ports on the valve. We were using a 10-port valve, with one port assigned to the bypass mode and 9 available for samples. We opted to only utilize 8 of those ports because it was convenient to store the resulting filters in 8x12 sample trays. Sampling interval duration depended on sample flow conditions and particle densities, which determined when the automated stopping criteria were reached. The period in between filtrations can also be user defined, based on the desired sampling density and time needed to remove samples and load new filters.

We also added controls to accommodate taking replicate samples. When a replicate sample was requested by the user, the program proceeded immediately from the first to second filter with no time break. This approach only produced a real replicate when the source water was not changing within the sampling time period, otherwise, exact replication was not possible. We also designed additional controls to allow a run to be manually stopped or a sample to be skipped if necessary.

The SAFS was designed with the intent of coupling it to a towed/pumping profiling vehicle (e.g., Hales and Takahashi, 2002) that sampled the water column at relatively high speeds (up to 1.5 m/sec). Therefore, minimizing sampling time was a priority. Longer sampling intervals would integrate larger portions of the water column, hindering our ability to determine high-resolution spatial/depth patterns in POC distributions. Conversely, short sampling periods would result in lower particle content samples, lowering the analytical signal to noise ratio.

Optimizing the filtration period during sampling was an important objective of the SAFS design. To that end, parameters were added to allow the program to adapt to different particle concentrations. The rate of flow through a filter depends not only on the line pressure, but also on the particle loading of the filter. As such, a decrease in flow rate should be indicative of substantial particle loading. We designed the program to take an average of the bypass flow rate (measured once per second) for 20 seconds prior to the beginning of each sample, and then subtract the average flow rate between the 20th and 30th seconds after the valve switches from bypass to a filter. We assumed that large differences between these two flow measurements, equivalent to a drop in flow rate >30%, were indicative of high POC loading. If these conditions were met, the program automatically decreased the sampling time-interval and flow-volume criteria for terminating the sampling event. Otherwise, the program continued to use the primary set of parameters.

The program was designed to log all operational data – time-stamp, flow rate, current integrated flow-volume, and sample number - at half-second intervals for each complete sample interval. In addition, processed data for each individual sample—time-stamp, sample ID, and total flow-volume—were logged separately. Each complete sampling sequence produced two time-stamped files, one containing the raw half-second data, and one containing the processed results, for all individual samples in a run. Table 1 in Appendix A shows an example of the logged data. All time-stamps recorded coordinated universal time (UTC), which was used for all other shipboard and *in situ* measurements and allowed for the direct comparison of POC data with all other measurements.

2.2. Sampling Methods – 2008

Once the apparatus was built and the programming was completed, we performed a series of laboratory and field tests to confirm the reproducibility and accuracy of samples collected by this method with those collected by traditional manual filtration. All samples for these tests were collected during the summer of 2008 from different sites along the central Oregon coast. This allowed us to both test the system and to evaluate the POC concentrations in this region of the Oregon upwelling system, which we used to determine the volume of water needed to exceed analytical detection limits.

2.2.1. Setting

The research site for both 2008 and 2009 was on the Oregon coastal margin between 43.8º and 45.4ºN. During the summer, wind-driven upwelling fuels high levels of production in this region. Upwelled water outcrops within 5-6 km of the coastline, shoreward of the 50m isobath (Allen et al., 2005; Kirincich et al., 2005). The bottom boundary later is the primary pathway for upwelled water to reach the euphotic zone (Perlin et al., 2005) and nutrients supplied to the surface by this pathway fuel blooms of phytoplankton, primarily diatoms (Barth and Wheeler, 2005, and references therein). The Oregon coastal system also has periodic relaxation events throughout the summer, when the northerly winds driving Ekman transport die down for a few days. Some of these relaxation events are strong enough that Perlin et al. (2005) found that near-bottom water can move seaward across most of the continental shelf before the winds reinvigorate upwelling. The bathymetry of this segment of coastline varies significantly (see Figure 2). At the northern end of the study area, the shelf is narrow and depth contours are evenly spaced and parallel to shore. The shelf broadens dramatically southward forming Heceta Bank, an area characterized by highly variable bathymetry and an abrupt shelf-break with a steep slope that drops precipitously to depths approaching 1000m.

2.2.2. Laboratory Tests

On June 13 and July 18, 2008 we collected water samples from both the near-surface and near-bottom waters at several stations on two cross-shelf transects near (the 'NH line') and just north of (the 'LB line') Newport, OR (see Figure 2). The surface samples were collected using a clean bucket, while the near-bottom samples were collected with Niskin bottles during CTD casts. The water was stored in clean

Nalgene bottles and/or collapsible 10L carboys and stored in the dark in coolers for transport back to the lab.

In the lab, each sample was simultaneously filtered using both manual and automated methods. We used a peristaltic pump and a recirculation line from the sample reservoir to create flow through the SAFS, while we vacuum filtered the manual samples. The volume of water filtered varied between the sampling locations and periods due to differences in particle concentrations. In June we filtered 200-500 mL, while July particle concentrations were sufficiently high that we only filtered 150-300 mL. For a given sample, we generally filtered the comparable volumes of water with each method.

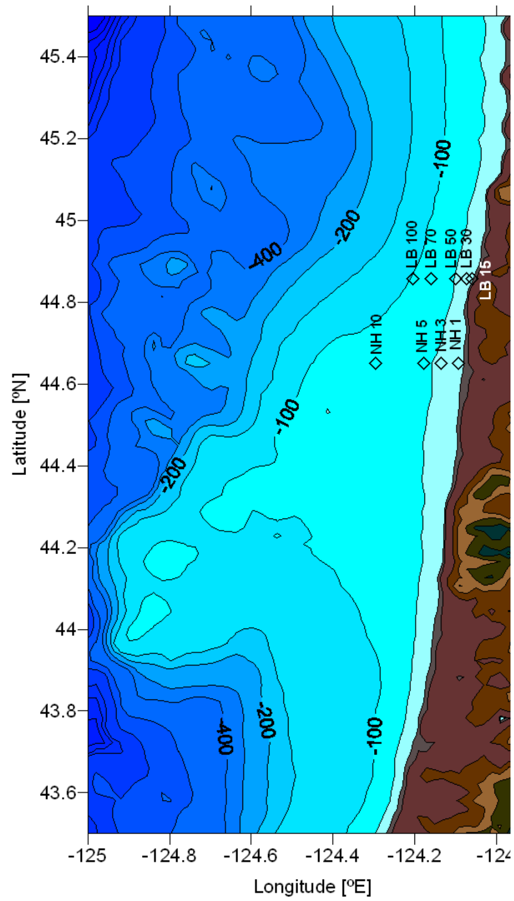

Figure 2 – Locations of NH and LB stations off of the Oregon coast.

2.2.3. Field Testing

In September 2008, we deployed SAFS on a ship (*R/V Wecoma*) for the first time. The SAFS was coupled to a flow of water pumped to the ship via the SuperSoar, a towed vehicle that is a modification of the Lamont Pumping SeaSoar, described in Hales and Takahashi (2002). Briefly, the SuperSoar carries a sampling pump that delivers water at ~8 L min^{-1} to the shipboard laboratory via a tube in the core of the tow cable. The vehicle carries a suite of hydrographic sensors (bio-optical and CTD) for *in situ* measurements, and actively controls its depth through a combination of winch control and adjustment of dive planes. We plumbed the SAFS to a branch of the shipboard end of the SuperSoar sampling line using 1/8" PEEK tubing, and found that line pressure was sufficient to drive adequate flow through our system.

To compare the manual and automated methods during this cruise, we sampled from the SuperSoar line at a fixed location when the SuperSoar remained at ~50 m depth for over 20 minutes, allowing us to collect multiple automated 100 mL samples from approximately the same water mass. Simultaneously, we collected a large volume of water (~ 10 L) from the main SuperSoar flow line. We homogenized the sample and filtered 185 mL of water manually onto each of eight 13mm filters under vacuum. All of these samples were stored frozen until analyzed as described for the in-lab samples.

On September 10, we connected the SAFS's intake to the ship's surface-underway sampling line to collect samples during a 10-hour steam along the track illustrated in Figure 3. The surface intake system in the Wecoma draws water from approximately 5m depth and is equipped with sensors that measure salinity and temperature, chlorophyll fluorescence and optical beam attenuation (c_p). The optical measurements were averaged across the time of automated POC sampling to end up with directly comparable data sets.

We sampled during a ~10-hour transit on September 10 from 03:20-12:45. The ship started at 45.35ºN and

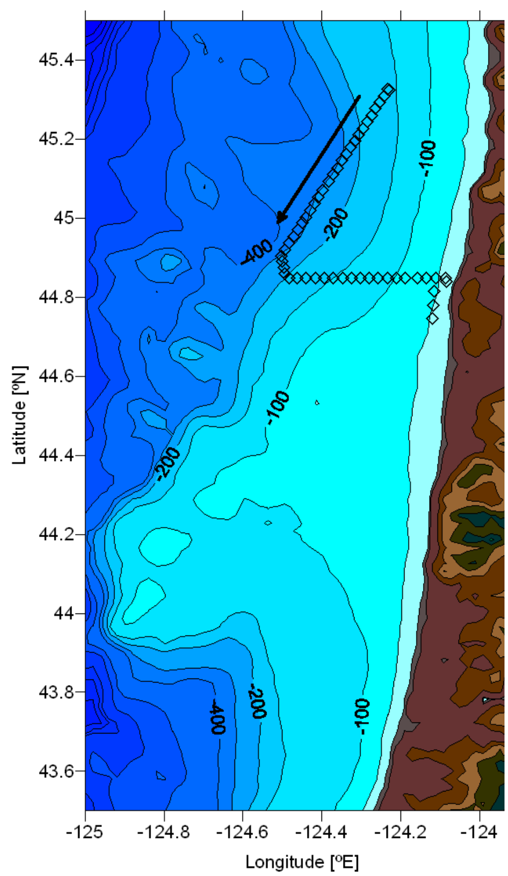

Figure 3 –The ship track followed during the transit on September 10. Every diamond represents one POC sample collected.

headed southwest along the shelfbreak until reaching 44.85ºN, at which point it turned due east and steamed across the shelf towards port. The SAFS was set to begin collecting a sample every ten minutes. The desired volume to sample was 100 mL, with a maximum sampling time of 2 minutes, and a minimum flow rate of 30 mL/min. At the time of this deployment, we had not yet added the high particle load protocols to the program, so all samples were collected with the same settings. All filter samples were frozen and processed in the lab for POC and PN content by the method described below. During this field deployment, we periodically checked the flow sensor volumetrically, verifying that it held its calibration throughout this operation.

2.3. Sampling Methods - 2009

2.3.1. Field Deployment

In May of 2009, we returned to the same area of the Oregon coast to collect samples using the SAFS. Over the course of two weeks, we sampled from a section of the continental shelf, bounded on the North and South by the 45º and 43.9ºN lines of latitude, and on the East and West by the shoreline and the continental shelf break. During these cruises, we sampled water using a different towed vehicle, the SuperSucker (described in Hales et al., 2004; 2005), rather than the SuperSoar. The SuperSucker is designed to operate at

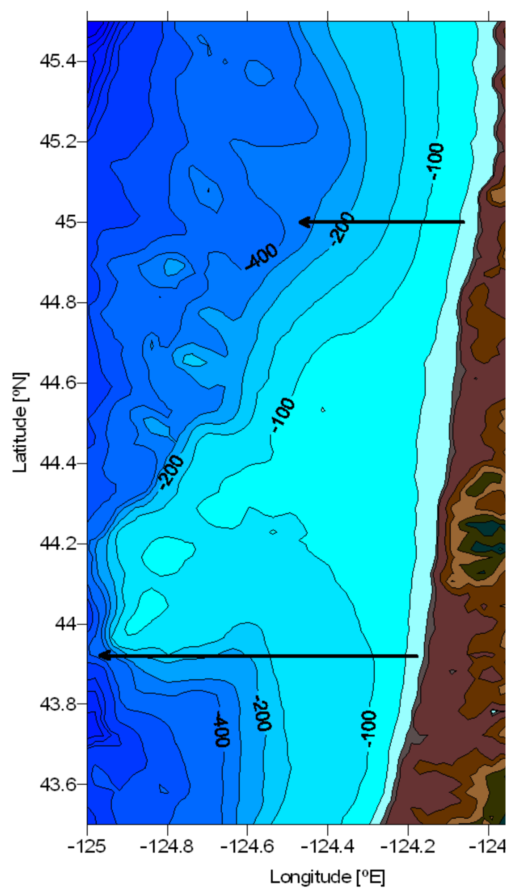

Figure 4 - Map showing the two transect lines followed during the May, 2009 cruise.

low speeds under winch-control alone, and gives more precise position control, desirable for the near-bottom focus of the cruise. All other aspects of the *in situ* sensing and sampling of the SuperSucker relevant to the POC collection are the same as the SuperSoar. The instruments on board the SuperSucker collected a suite of *in situ* measurements including temperature, salinity, beam-c, optical backscatter, and chlorophyll fluorescence.

During this cruise, we performed focused water-column surveys along two East-West transect lines, one at 45.0º N and one at 43.9ºN (Figure 4). During these transects, the ship towed the SuperSucker at a speed of ~1.5 kts, as the automated winch control raised and lowered the vehicle through the water column.

Flow through the filtration system was about 100 mL/min. POC concentrations during this cruise appeared to be relatively low, so we opted to filter 150mL of water per sample, resulting in a sampling interval of about 90 seconds. This increased the portion of the water column sampled by a single filter, but decreased the likelihood that samples would be below detection limits after corrections for filter blanks.

In addition, large volume samples (1000-3000 mL) were collected from both the ship's surface intake and the SuperSucker sampling lines. Because of the time required to manually filter these volumes of water, we collected large volume samples every hour. These water samples were manually filtered under a vacuum onto pre-combusted, pre-weighed 47mm GF filters for total suspended sediment (TSS) and stable isotope analysis. Each sample was rinsed with deionized water after sampling to minimize increases in mass due to salt retention. The filters were frozen until they could be analyzed in the laboratory.

2.3.2. Lag Correction

In order to correlate the POC samples we collected with *in situ* data, we had to correct the time stamp associated with each sample for the amount of time required for water to travel through the tubing from the SuperSucker to the filtration system.

The appropriate correction was found by comparing two time series of salinity, one measured on the vehicle and one measured in the sample stream aboard the ship (following Hales and Takahashi, 2002).

The filtration system was significantly up stream of the shipboard instrument that provided the salinity readings, therefore we had to perform an additional time correction to account for the sample lag between that sensor and filtration system. This lag was assumed to be proportional to deviations in the total lag at the shipboard salinity sensor relative to some minimum lag time for the water to reach the ship. The additional lag to the SAFS is some fraction of the difference between the total and minimum lags. Since POC and optical beam attenuation are highly correlated (*i.e.* Karp-Boss et al., 2004), we were able to refine the lag correction between the shipboard sensors and the SAFS by minimizing the variability in the correlation between the two properties. Once the POC sampling times were corrected for lag, the data for each of the high-resolution measurements within that interval were averaged for direct comparison to the POC numbers.

2.4. Analytical Methods

2.4.1. CN Analysis

POC and PN (particulate nitrogen) analyses of filters were performed according to established methods (e.g., Goni et al., 2003). Briefly, after sampling filters were placed in 8x5mm silver boats and loaded into a desiccator where they were exposed to concentrated HCl vapors for 24 hours. The desiccator was vented for 20-30 minutes after the acid was removed, then loosely covered with aluminum foil, and placed in a 50ºC oven for at least 48 hours. Once the samples were dry, the silver boats were carefully folded with clean forceps and placed into 8x5mm tin boats. The tin boats were then folded firmly around the sample to form a small ball. The folded samples were analyzed for C and N content by high-temperature combustion in a Thermo Quest EA2500 Elemental Analyzer. Helium gas was used as the carrier while the combustion and reduction ovens were kept at 1030ºC and 753ºC, respectively. Varying weights of cystine, atropine, and a low-carbon sediment standard were used to create a five-point calibration curve every time the instrument was run. In addition, pre-combusted filter blanks were acidified and wrapped in silver and tin boats to account for the C and N content of the filters. Tin boat blanks and filter blanks were also analyzed as an additional check within each EA run. Particulate organic nitrogen (PON) can be determined from the resulting data by assuming that all PN associated with POC is PON. A positive intercept in the relationship can indicate contributions from inorganic nitrogen adsorbed onto particles and must be corrected for.

2.4.4. TSS and $\delta^{13}C$ Analysis

The large volume filter samples collected manually were used to determine the concentration of total suspended solids (TSS) and the stable isotopic composition of the particulate organic matter. All of the 47mm filters were dried in a 60º C oven for 24 hours. A subset of samples was selected for stable isotope analysis. Each 47mm filter was sub-sampled using a solvent-cleaned hole-punch. Several sub-samples were taken to obtain sufficient material for isotope analysis. The filter punches were placed into 8x5mm silver boats. A drop of DI water was added to each boat to help facilitate acidification. All samples were acidified, dried, and balled using the same method as described for elemental analysis. Stable carbon isotopic compositions of organic matter ($\delta^{13}C$) collected in filters were determined using a Carlo Erba Elemental Analyzer interfaced with a Finnigan Mat Delta Plus-XLS isotope ratio mass spectrometer by a Conflo-III system according to Goni et al. (2005) and reported in the usual δ per mil (‰) notation vs. PDB. Isotopic standards with contrasting isotopic compositions, including cystine, leucine, acetanilide, sucrose, and ammonium sulfate, were run each day to calibrate the instrument.

3. Results

3.1. –2008 Tests

3.1.1. Laboratory Tests

POC concentration of surface samples (Figure 5a) filtered manually ranged from 8.94-55.0 µM with standard errors ranging from 0.57-3.7 µM. The samples collected using the semi-automated system ranged from 4.33-49.7 µM, with uncertainty of 0.087-1.4 µM . The near-bottom (Figure 5b) manually filtered samples ranged from 10.9-21.3 µM with 0.27-3.4 µM uncertainty. The automatic samples ranged from 6.10-25.7 µM with 0.36-4.5 µM uncertainty. These results show strong correlation (slope = 0.97±0.07, R^2 = 0.93) between the two sampling approaches, with a possible systematic offset around 2 µM (Figure 6). Analysis of replicates indicates that the samples collected by the automated system have analytical uncertainty that is similar

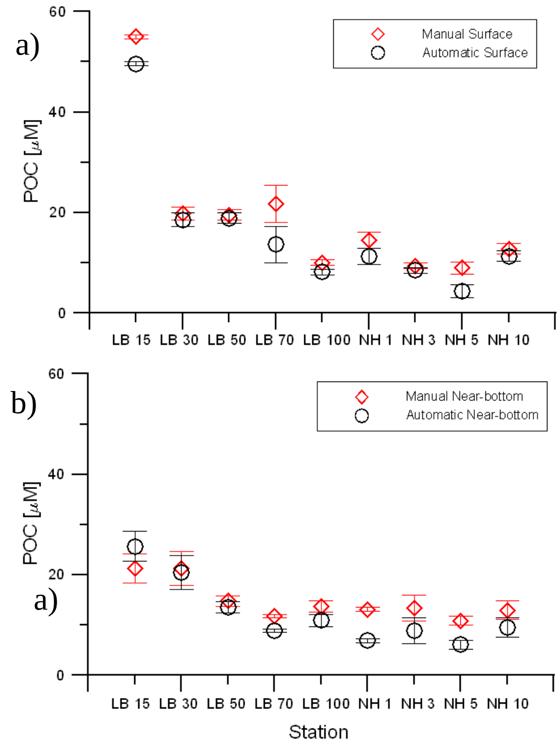

Figure 5 – July results for manual versus automatic samples taken on the LB and NH sampling lines at both the surface (a) and the near-bottom (b).

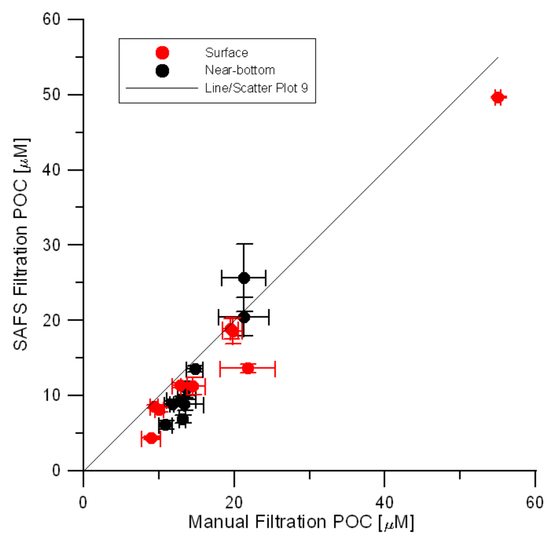

Figure 6 – Comparison of SAFS and manual POC results from July 2008 NH and LB samples.

to manually collected samples. Both methods captured the same cross-shelf and surface to bottom trends, indicating that the semi-automated system is a viable method for collecting particulate organic carbon samples over a range of conditions.

3.1.2. Field Tests

We performed additional testing during a field experiment in September 2008 based on manually and automatically drawing and filtering samples from the ship's surface intake line, and from the sample stream delivered by a pumping/profiling sampling vehicle. In the first case, we collected several replicate samples by each filtering approach while the towed vehicle was at a fixed depth in the water column. Real variability in the sample stream combined with temporal mismatches in the two sampling approaches made it difficult to sample true replicates by the two different methods, but average concentrations and dynamic ranges were quite similar. POC concentrations in the manual samples ranged 13.8-17.0 µM, with a mean of 14.8±0.4 µM (n = 8). The automatically collected samples had POC concentrations ranging from 12.6-18.6 µM, with a mean of 14.5±1.0 µM (n = 6). In each case, the observed variability was similar to expected analytical uncertainty. We performed an ANOVA on this data, and found no statistical differences between the manual and semi-automatic filtration methods.

In the second case, we collected multiple samples from the ship's surface intake line as we steamed first to the SSW along the shelfbreak, and then across the shelf to the nearshore (Fig. 4). The data for this transit are summarized in Figures 7-9 and Appendix C. The POC data show that during the first two hours of the transit we crossed a strong gradient in surface POC concentrations, which decreased from ~80 µM to 10 µM (Figure 7a). This drop in POC corresponds with a proportional decrease in chlorophyll fluorescence (1.268 to 0.300 V, Figure 7b) and beam attenuation coefficient, c_P (2.6 to 0.8 m^{-1}, Figure 7c). Subsequent to the decline in particle load in the water, smaller features present in the c_P and fluorescence signals are also detectable in the POC data. Both POC and optical measurements remained low until the last two hours of the transit, at which time all values began to increase again near shore. These data show highly significant, positive, linear correlations between both optical measurements and POC (Figure 8).

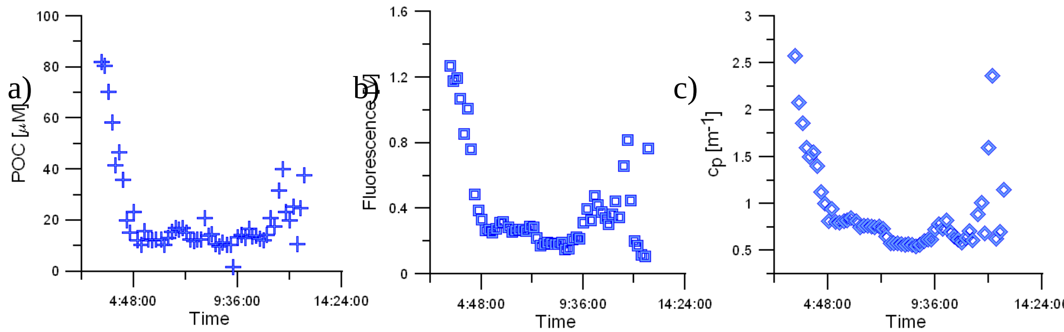

Figure 7 – Distribution of surface-water (a) POC [µM] (b) chlorophyll fluorescence (uncalibrated sensor voltage, V), and (c) beam attenuation coefficient, c_p [m^{-1}], plotted against time during the September 10 transit.

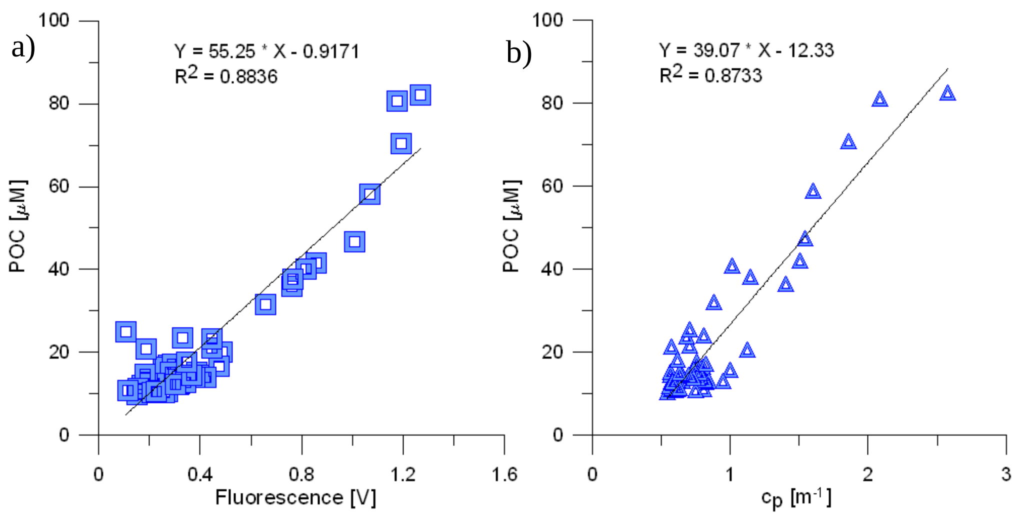

Figure 8 – POC concentration [µM] versus chlorophyll fluorescence [V] and beam attenuation coefficient (c_p) during the September 10 transit.

Examination of the temperature and salinity data along the transect line (Figure 9) show that the ship moved through a variety of water masses along the transit. Initial conditions consisted of relatively salty and cool water, indicative of upwelling-influenced shelf water. We subsequently crossed through warmer fresher

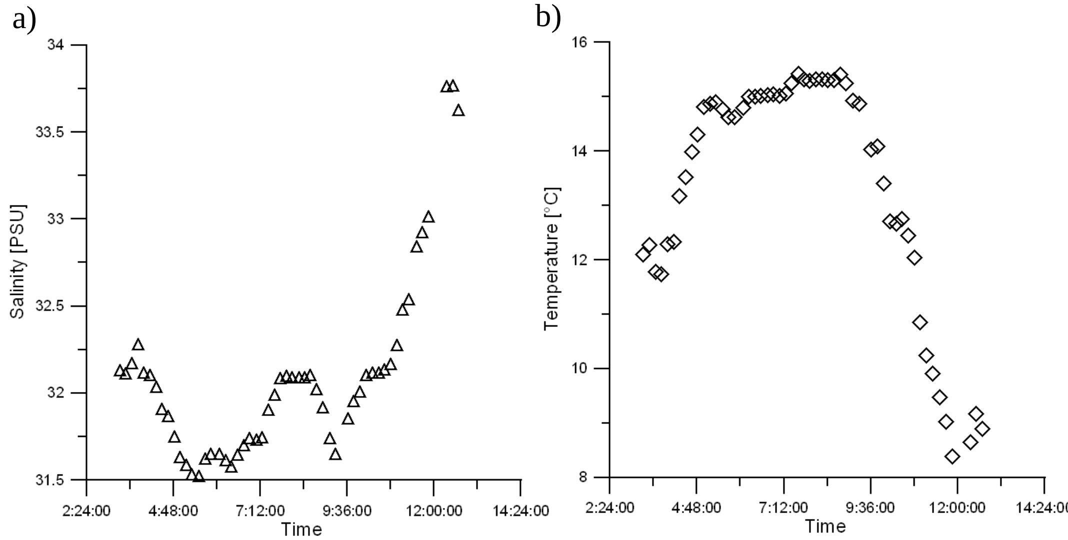

Figure 9 – Distribution of (a) salinity (PSU) and (b) temperature (ºC) against time during the September 10 transect.

waters, and then through warmer waters with relatively high salinity, suggesting interaction with modified Columbia River plume and offshore North Pacific surface waters. Upon turning to the East and steaming across the shelf, surface waters became dramatically colder and saltier, indicative of upwelled source waters in the nearshore. Coincident with the T, S signatures of upwelled source waters were high POC, fluorescence, and c_p values, consistent with elevated contributions of phytoplankton biomass resulting from upwelling-driven production. As the ship moved offshore and out of the colder water mass, POC, fluorescence and c_p abruptly decreased to values of 10 µM, 0.2 V, and 0.75 m^{-1} respectively (Figures 7 and 9), indicative of low algal biomass.

3.2. Field Results - 2009

3.2.1. POC profiles

During late spring of 2009, we operated the SAFS interfaced with the SuperSucker towed profiling sampling vehicle described in Hales et al. (2005; 2006). We present here results from two cross-shelf sections from a region of simple bathymetry and narrow shelf width at 45ºN, and a broad-shelf region of complicated bathymetry at 43.9ºN. On the southern transect, we collected 239 particulate organic carbon samples over a 22-hour period, while on the northern transect we collected 100 samples over an 8-hour period. For comparison, collection of a similar number of samples would have required hourly deployment and sampling of a 12-bottle CTD rosette along these sections to yield similar sampling density. In the south, concentrations ranged from 0.417 to 116 µM, while in the northern section the dynamic range was smaller, ranging from 0.836 to 38.8 µM. Once the POC data was correlated with the *in situ* data, we plotted cross-sections of the results (Figure 10).

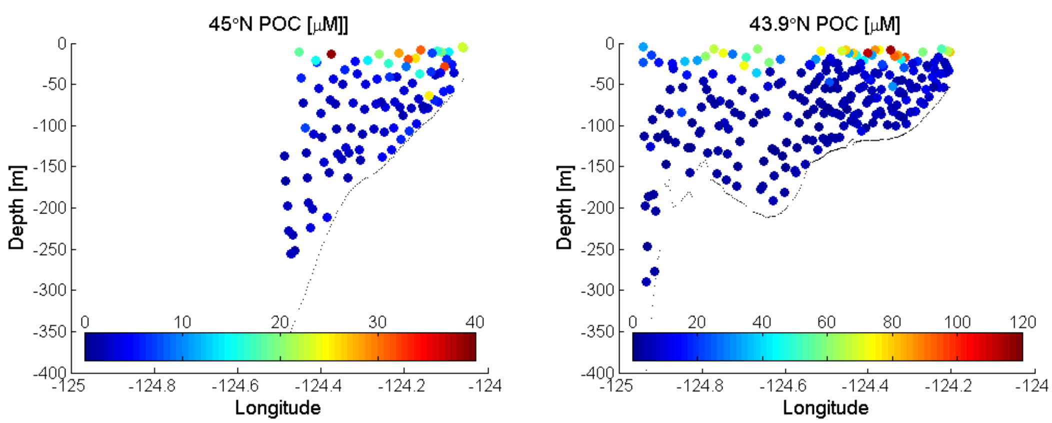

Figure 10 – POC distributions along 43.9º and 45ºN transects in late May 2009.

Since there are still relatively few individual measurements, we did not use any type of gridding to interpolate the data, and the location of each sample is based on the average depth and longitude over the sampling period. Appendix C contains a table of all the POC results and corresponding *in situ* measurements, as well as cross-section plots depicting the full range of water column sampled.

The POC distributions show elevated concentrations of organic carbon in the surface water of both transects, with peak POC concentrations just seaward of the upwelling pycnocline, consistent with previously observed surface productivity patterns (e.g. Small and Menzies, 1981; Hill and Wheeler, 2002; Karp-Boss et al., 2005; Hales et al., 2006). In addition, slightly elevated POC concentrations were measured in a few mid-water and bottom boundary layer samples, which were clearly different from areas of elevated surface concentrations (see Appendix C.2.).

3.2.2. Optical Results

Cross-shelf distributions of *in situ* optical measurements (Figure 11) show consistent patterns. Beam-c shows elevated values in surface waters, with an additional slight elevation in the bottom boundary layer. Chlorophyll fluorescence is also elevated in the surface, but low in the rest of the water column with no corresponding BBL enhancement. The chlorophyll and c_p signals indicate an abundance of phytoplankton in the surface that is strongest near shore and extends seaward to the 200m isobath, echoing the POC results shown in Figure 10. Optical backscatter, nominally related to total particle abundance, also shows elevated signals in near surface and near-bottom waters, but the near-bottom signals are higher in comparison to the surface values relative to what was observed for the other two optical proxies. Structure in these optical properties is similar for each transect, although surface signals are smaller at 45ºN than at 43.9ºN. (Plots of the temperature and salinity profiles are in Appendix C.3.).

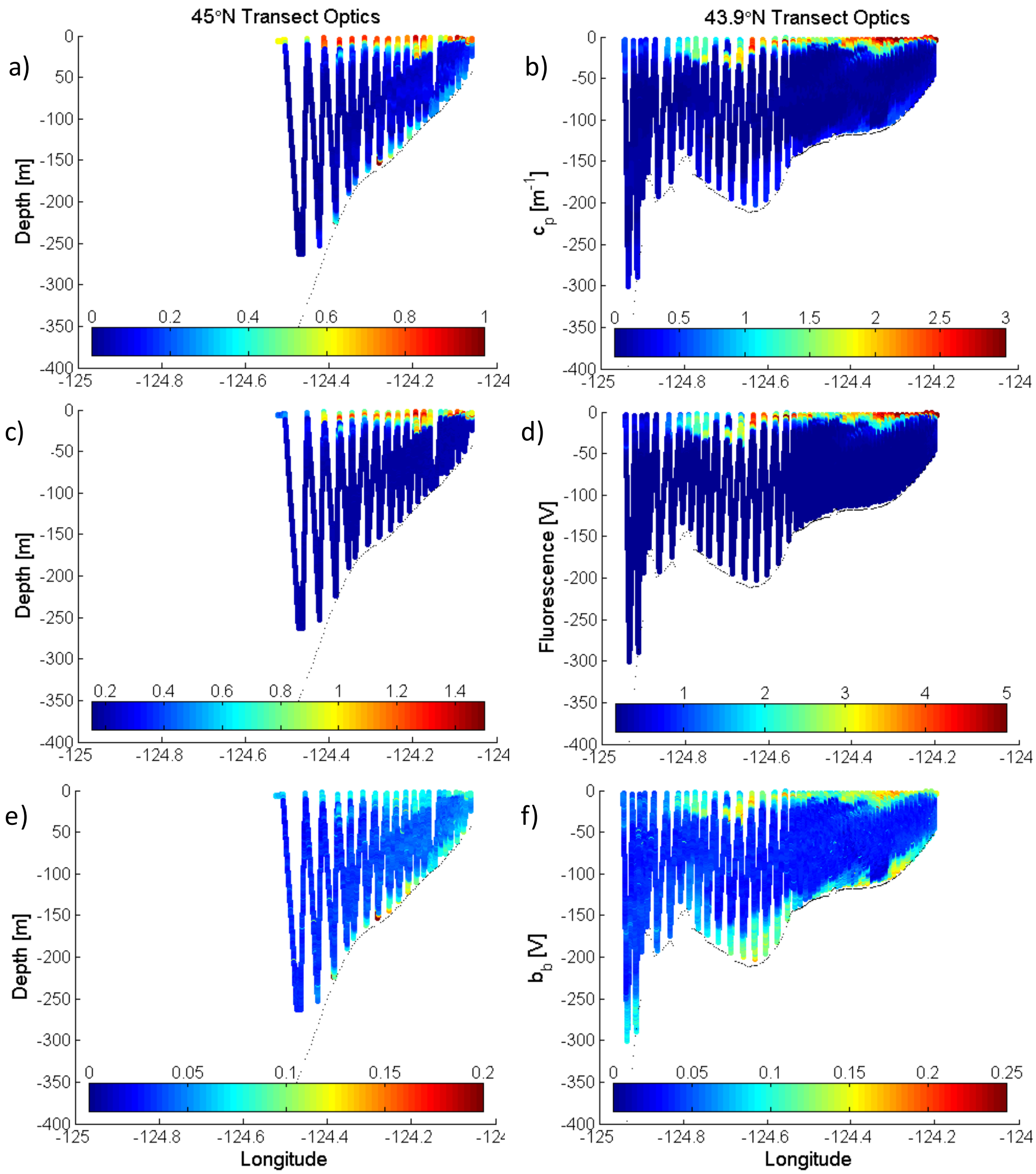

Figure 11 – High-resolution optical measurements from 45ºN and 43.9ºN transects, a-b) optical beam attenuation (cp), c-d) chlorophyll fluorescence, and e-f) optical backscatter.

3.2.3. POC-optical correlations

The trends in measured POC are coherent with the optical beam attenuation data. The POC samples from the 43.9ºN transect correlate strongly to c_p ($R^2 = 0.90$), with a slope of 50±2 (Figure 12b), in agreement with the findings of Karp-Boss et al., (2004). The samples from 45ºN have a dynamic range that is about 1/3 of the 44ºN samples for both measurement, and consequently the correlation is not as strong (R^2 = 0.60, slope = 39±4), but still significant (Figure 12a).

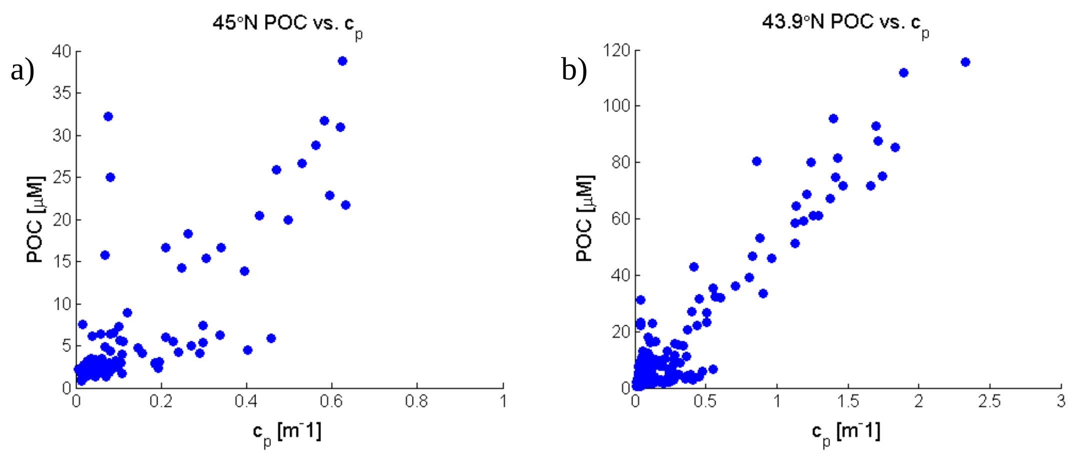

Figure 12 – POC concentrations plotted again optical beam attenuation for a) the 45ºN transect and b) the 43.9ºN transect.

Property-property plots of beam attenuation versus optical backscatter clearly show two distinct particle pools (Figure 13, on the following page). One pool is rich in POC and shows elevated beam-c and fluorescence (see Appendix C) relative to optical backscatter, while the other is depleted in POC and shows proportionately elevated backscatter. Smaller inorganic particles have proportionately higher backscatter signatures relative to beam attenuation due to a combination of size and refractive index (Boss et al., 2001; 2004; Gardner et al., 2001). This suggests that the latter pool is highly degraded and may be remnant of winter-source material, while the former is probably recently produced phytoplankton-derived material.

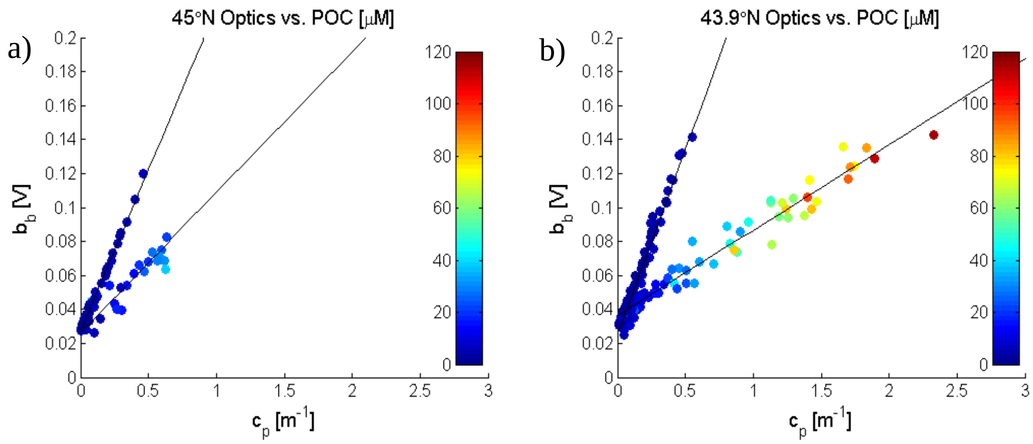

Figure 13 – Plots of optical properties from a) the 45ºN transect and b) the 43.9ºN transect. POC concentrations are shown as the color scale in both figures.

The two pools distinguished by the backscatter-c_p relationship appear to be consistent from one transect to another. Looking at the correlation statistics in Table 1, the most obvious difference is the change in slope from one surface pool to another. However, there is a large amount of uncertainty in the 45ºN surface pool slope, driven by the reduced dynamic range and small number of samples compared to 44ºN. There is a slight difference between the slopes of the two BBL pools, although those relationships are more tightly correlated and have much narrower confidence intervals.

	Slope [V*m]	Intercept [V]	R^2
45ºN Surface	0.08±0.03	0.03±0.01	0.62
45ºN BBL	0.190±0.005	0.0273±0.0006	0.99
43.9ºN Surface	0.051±0.004	0.036±0.0035	0.93
43.9ºN BBL	0.218±0.008	0.025±0.002	0.95

Table 1 – Slopes, intercepts, and R2 of the correlations between backscatter and beam-c seen in Figure 13, with 95% confidence intervals.

3.2.6. Optical Ratios

Optical ratios were calculated from unit-normalized values of fluorescence, optical backscatter, and beam-c. Each measurement was transformed from the absolute observed ranges in either raw voltage (in the case of fluorescence and optical backscatter) or beam-c to relative scales from 0-1 by subtracting the minimum value from each sensor, and dividing that blank-corrected value by the sensor's dynamic range. Noise levels were determined for each instrument by calculating the standard deviation signal observed during instances of relatively constant, near-zero readings. Ratios were only calculated when absolute measurements that were greater than five standard deviations above the minimum observed value for both fluorescence and backscatter. We raised the threshold for beam-c measurements to ten times the noise level because that term was used primarily in the denominator of our ratios and we wanted to avoid interpretation of large signals that may have been the result of dividing by numbers near zero. In addition, during the 44N transect, the high chlorophyll levels maxed the fluorometer's response at 5V. Since these data are not meaningful for optical ratios, we also eliminated data within the noise threshold of the fluorometer maximum. The resulting high-resolution distributions are plotted in figure 14.

These plots show areas of elevated fluorescence and backscatter relative to c_p (> 2.0 for both measurements) distinct from either surface or BBL pools, suggesting a unique mid-water particle mass. Fluorescence:c_p is also elevated within surface waters (> 1.0), as expected for photosynthetically-active phytoplankton assemblages, and low within the bottom boundary layer (<0.5). Conversely, backscatter is depleted relative to c_p (b_b:c_p<1.0) in surface waters and somewhat elevated (between 1.0 and 3.0) in the bottom boundary layer.

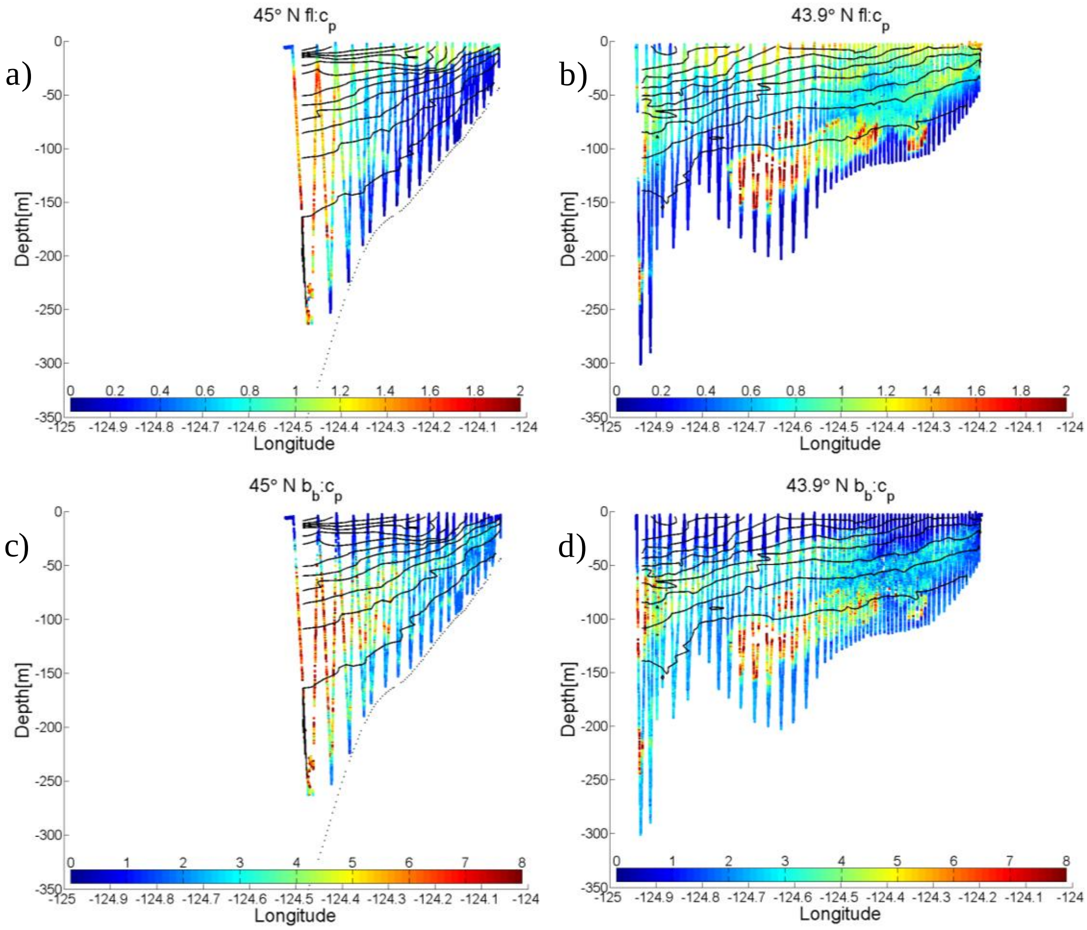

Figure 14 – Ratios of a-b) chlorophyll fluorescence to optical beam attenuation, and c-d) optical backscatter to optical beam attenuation along the 45º and 43.9ºN transects. The isopycnal contours on the 45ºN plot range from 26.5 to 23.0, and on 43.9ºN range from 26.5 to 24.25.

In order to compare these optical ratios to POC concentrations, ratios were also calculated using the same methods described above for each POC sample (see Appendix C for cross-section plots). Combining the optical ratios with the POC-c_p relationship (Figure 15) yields segregations of several particle pools within the water column. The BBL pools are clearly distinguished by very low levels of fluorescence to c_p (Figure 15a&b), while the surface pool shows low backscatter relative to c_p (Figure 15c&d). A third pool can be distinguished as having elevated values of fluorescence, backscatter, and POC relative to c_p measurements.

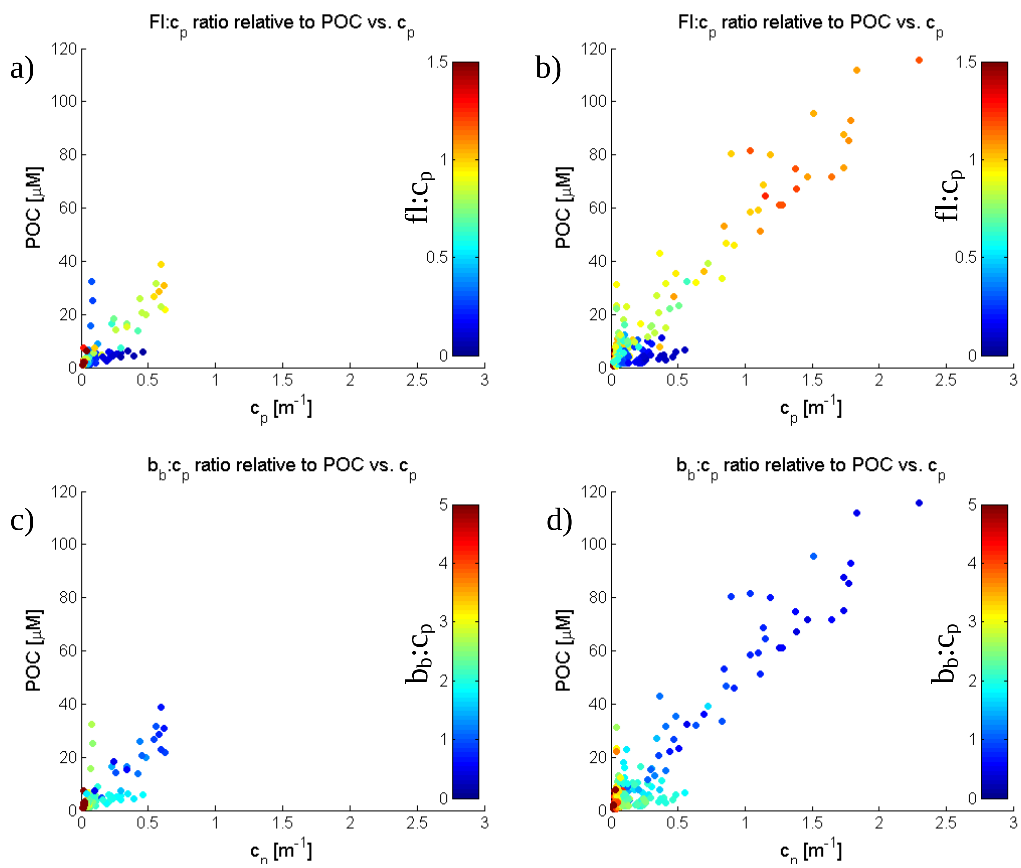

Figure 15 – Optical ratios as relate to POC [μM] and c_p [m^{-1}]: a-b)chl fl:c_p, and c-d) b_b:c_p at both 45° and 43.9°N.

3.2.4. Blank Considerations

Due to the small amount of material collected on each filter, the POC data have a low signal to noise ratio, warranting extra consideration of the blank for each sample. Sampling a wide variety of water masses containing dramatically different particle pools makes determining an appropriate blank correction difficult. Here we consider two primary factors relevant to the sampling method used: 1) the carbon content of the glass fiber filter, and 2) DOC adsorption onto the filter.

Consistently accounting for the carbon content of combusted GF filters for the samples from 2009 took some consideration, given the large number of samples to be analyzed. There is inherent variability in the carbon content of glass fiber filters, but in addition, the filter used were combusted at different times and stored in multiple glass vials. 8-16 blanks were stored and frozen in every sample tray during the cruise. In order to capture blank variability, 57 blank filters were analyzed as samples in the EA for carbon content. A few filters were analyzed from each of the different sample trays. In addition, we analyzed two blank filters with every 35 samples analyzed. The average carbon content of the 108 blank filters analyzed was 0.28±0.10 µmoles C, and this value was used to blank correct all of the samples from May 2009 (Table 2 contains a summary of the GF and DOC blank correction values discussed here). These values are significantly above the analytical detection limit of our instrument (0.04 µmoles C), allowing us to confidently constrain the carbon contribution from the filters themselves. Given the amount of variability within filter blanks, our detection limit is 2 standard deviations above the average, or 0.48 µmoles C . Of the 339 samples collected during the May transects, only 16 fall below 0.48 µmoles C/GF. All of the samples have been corrected for the average carbon content of a blank filter (0.28 µmoles C).

Due to the minimal amount of particulate collected for most samples, PN values were at or below detection limits for the majority of our samples. Consequently, we do not report any PN or (OC:N)a data for these transects.

Source	Values		
	25mm GF umoles C	13mm GFF umoles/GF	mg/GF
GF Blank			
GF Blank Average		0.28±0.10	0.0034±0.0012
Anayltical Detection Limit		0.48	0.0054
DOC Adsorption			
Menzel (1966)	1.7-2.1	0.46-0.57	0.0055-0.0068
Moran et al. (1999)	2.0	0.54	0.0065
Laboratory Test	1.8-2.0	0.48-0.53	0.0060-0.0064
POC to c_p Correlation	0.37	0.10	0.0012

Table 2 – Approximate carbon content due to GF blank and DOC adsorption.

Correcting appropriately for DOC adsorption to glass fiber filters is difficult under the best circumstances. POC studies in the past have used a variety of approaches for approximating a DOC correction (Loder and Hood, 1972; Moran et al., 1999; Gardner et al., 2003). Due to the large number of samples collected, stacking a second filter for each sample, as in Loder and Hood (1972), was impractical from both a logistical and analytical standpoint. Alternatively, in late August we acquired 10L of surface water from within the area we sampled earlier in the summer. This water was thoroughly homogenized, then filtered through 13mm GF filters by manual filtration. We collected the filtrate in clean glass containers, homogenized it, and filtered this "particle free" water through clean 13mm GFs at volumes ranging from 50-600mL. All of these samples were frozen prior to analysis. The filters were acidified and analyzed by the same method described in section 2.4.1. The GF filtrate results show that between 100 – 150 mL, the range of volumes of nearly all our field samples, between 0.48-0.53 µmoles adsorbed to the filters (Table 2).

Moran et al. (1999) performed tests for DOC content by collecting a large volume of water from one oceanic site and filtering that homogenized sample at increasing volumes. The positive intercept from the resulting relationship between carbon content per filter and volume sampled is indicative of the DOC content of the filters. They performed this test on water samples from around the world. Their results indicated that a DOC blank of ~2 µmole C was typical for small volume (100-600mL) samples filtered onto a 25mm GF. This corroborates findings by Menzel (1966). These results are summarized above in Table 2. Literature results were normalized to a 13mm diameter filter for comparison to our results.

Given the linear relationship typically observed between POC and c_p (e.g., Karp-Boss et al., 2004), it follows that a positive intercept in the trend line may also be an indication of an average DOC blank within the sample set. In our data set from the 44ºN transect, the correlation between POC and c_p yields a positive carbon intercept at $c_p = 0$ of 0.6501 µM, with a 95% confidence interval ranging from -0.3962 to 1.696 µM (Figure 13b). This value is a concentration, however, so we convert it to a quantity of carbon per filter using the amount of water filtered (150mL), giving 0.10 µmoles C/GF.

Applying any of these test-derived DOC values to our entire data set has a significant inherent problem: the samples collected represent a wide range of different water masses, and were collected at different times and locations than either the literature values or laboratory test. For this reason, the POC data presented here is not corrected for a DOC blank. However, interpretation of extremely low carbon content samples (< 0.50 µmoles/GF, or ~3.5 µM) must reflect the potential influence of both variability in the GF blank and DOC adsorption.

3.2.5. Isotopes

Filters from the 43.9ºN transect were sub-sampled and analyzed for $\delta^{13}C$ composition. During each transect, samples were collected from both the surface intake and SuperSucker simultaneously. The surface samples range from -17.5 to -22.6 ‰. Sub-surface samples, taken from various depths in the water column, range from -19.8 to -24.3 ‰. The range in surface values varies with distance from shore; near-shore samples are significantly enriched in ^{13}C relative to those collected farther from the upwelling front, or from those collected in the sub-surface (Figure 16). The 45ºN transect, however, shows no significant gradient in the surface samples, which range from -19.9 to -21.1 ‰. Subsurface values have values similar to 43.9ºN, -21.0 to -24.5 ‰.

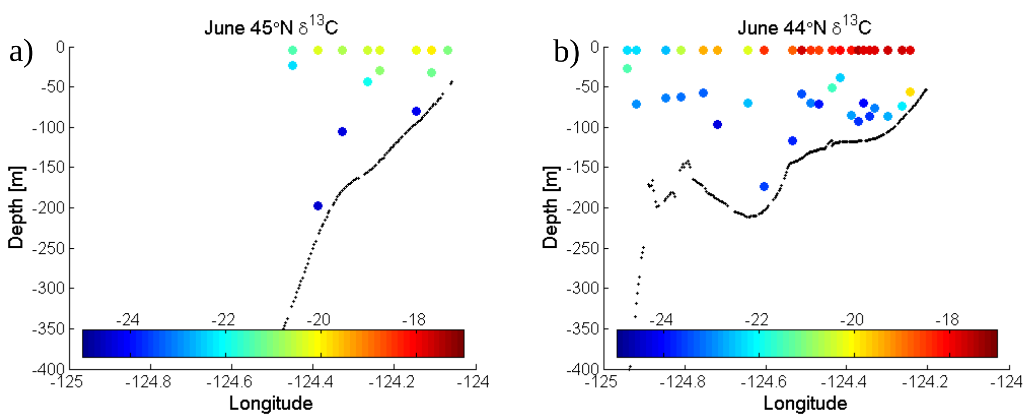

Figure 16 – Distribution of δ13C values within both the 45º and 43.9ºN transect.

4. Discussion

4.1. Carbon characterization

The optical properties observed during this study can provide insight into the characteristics of the particulate carbon throughout the water column. Variations in optical measurements are used to quantify a wide variety of particle properties, from phytoplankton physiology (Fennel and Boss, 2003; Eisner and Cowles, 2005; Behrenfeld and Boss, 2006) to particle size and composition (Boss et al., 2001; 2009; Loisel et al., 2007; Whitmire et al., 2007; Snyder et al., 2008), in addition to simple quantity abundances. Previous studies (Gardner et al., 2001) have also found distinct surface and bottom boundary layer particle pools distinguished by variations in optical beam attenuation and backscatter.

There is clear evidence of at least three distinct particle pools within our sample set (Figure 15), which can be roughly divided between the surface, mid-water, and bottom boundary layer. The surface water is dominated by large, fluorescent, carbon-rich particles, as evident by the elevated c_p and chlorophyll fluorescence. This pool, with carbon concentrations reaching 120 µM, is probably recently produced phytoplankton-derived material produced by large coastal diatoms (Small and Menzies, 1981). The mid-water column particles are small, as indicated by extremely low c_p signals and comparatively high backscatter and fluorescence. Particles in the bottom boundary layer are not as small as those in the mid-water, although backscatter is still elevated relative to c_p, but are extremely poor in both carbon content and chlorophyll fluorescence. The lack of chlorophyll and elevated backscatter suggest that this last pool is degraded and is dominated by inorganic particulate material (Boss et al., 2001; 2009), indicating that it may be remnant of the winter bottom boundary layer.

The stable carbon isotope composition of the surface particle pool further supports primary-production as the dominant source of POC. There is a strong off-shore gradient in isotopic composition, with enriched carbon near shore, which is typical of high productivity (Figure 16). Laws et al. (1997) and Woodworth et al. (2004) investigated the relationship between carbon fractionation (ε_p) and the ratio of inorganic carbon demand to supply in the laboratory and in the field respectively. Laws et al. (2004) found that the two properties are inversely related. In other words, under $CO_{2[aq]}$-limiting conditions, or at high phytoplankton growth rates, fixed carbon will be less fractionated and therefore enriched in ^{13}C. Woodworth et al. (2004) investigated the isotopic composition of organic carbon in sediment trap samples collected from multiple depths in the Cariaco Basin over three years. They found a direct correlation between the isotopic composition of POC and upwelling strength, which is consistent with Laws et al. (1997), and indicates lesser fractionation during conditions of very high production. The isotopic gradient we find moving seaward of the upwelling front along the 43.9ºN transect is consistent with a decrease in photosynthetic production, likely due to a decrease in nutrient availability.

In addition, Woodworth et al. (2004) found no significant isotopic fractionation in sinking particulate organic material. This implies that the isotopic composition is an indicator of source material rather than a result of degradation. Assuming that similar processes occur in the Oregon upwelling system, the relative isotopic compositions of the sub-surface POC samples are controlled primarily by the upwelling strength at the time that the carbon was fixed, several days prior to sampling.

4.2. Quantifying water column POC from c_p

Although the primary relationship between POC and c_p is consistent with previously reported relationships for this region (Karp-Boss et al., 2004), there is significant variability in the correlation, particularly at low values of POC (<40 µM) and c_p (<0.5 m^{-1}). The correlation between POC and c_p is dominated by signals from surface waters enriched in freshly produced phytoplankton material, which only comprise one of these particle pools. The three particle pools described in this study have distinct optical and particle properties, therefore applying the primary POC-c_p

correlation to the entire water column is not an accurate reproduction of POC distribution, and could result in erroneous estimates of the overall carbon content of the water column. Using optical ratios as defining parameters (Table 3), it is possible to segregate data into the different particle pools, and then apply an appropriate POC-c_p calibration to each, thereby producing a more accurate reconstruction of POC distribution. Applying these criteria (Table 2) to POC data collected from 43.9ºN, we get three distinct POC-c_p relationships (figure 17) with dramatically different slopes. We can then divide the high-resolution *in situ* optical data by the same method and apply the three calibrations described in Table 3. The resulting reconstruction of POC distribution has features that are distinct from a similar reconstruction using one simple c_p calibration (Figure 18).

	BBL	**Mid-Water**	**Surface**	**Combined**
fl:c_p	< 0.325	≥ 0.325	≥ 0.625	--
b_b:c_p	≥ 1	≥ 2.25	< 1	--
Slope	9.70	98.3	47.8	50.0
Intercept	1.55	2.08	6.58	0.650

Table 3 – Optical ratio limits used to define three particle pools for both determining POC-cp calibrations and segregating high-resolution measurements, and resulting calibration information for each pool. Also included is the calibration used for the simple POC reconstruction (Figure 20b).

The three-pool derivation of POC is different from the one-pool c_p derivation in two important ways. First, POC concentrations in the bottom boundary layer are significantly lower than those found using the one-pool method. Low POC concentrations coincident with elevated backscatter and c_p indicate a decoupling between particles and carbon in the BBL, particularly in comparison to those freshly produced in surface waters. Second, the mid-water column has areas of elevated POC, particularly off of Heceta bank. This suggests that the mid-water may be an area for advective transport of POC off the shelf.

a)

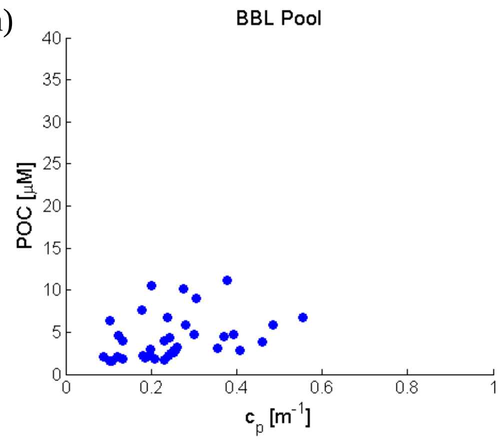

b)

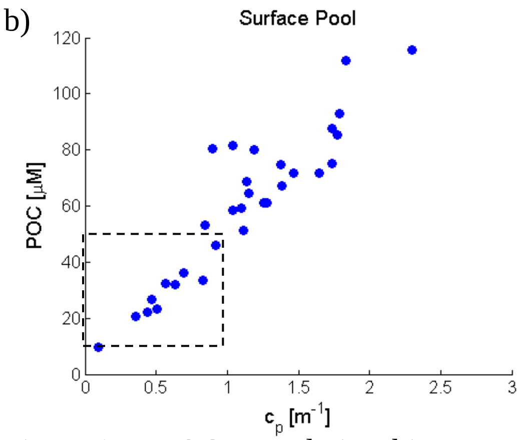

c)

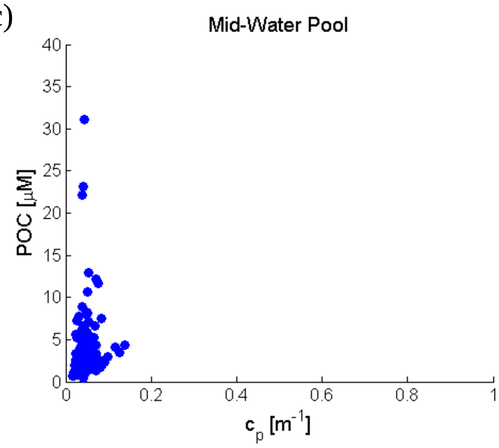

Figure 17 – POC - c_p relationships within the three particle pools: a) bottom boundary layer, b) surface, and c) mid-water (note different axis scales for BBL and mid-water). The resulting correlations provide three correlations from which POC concentrations can be derived (see Figure 18).

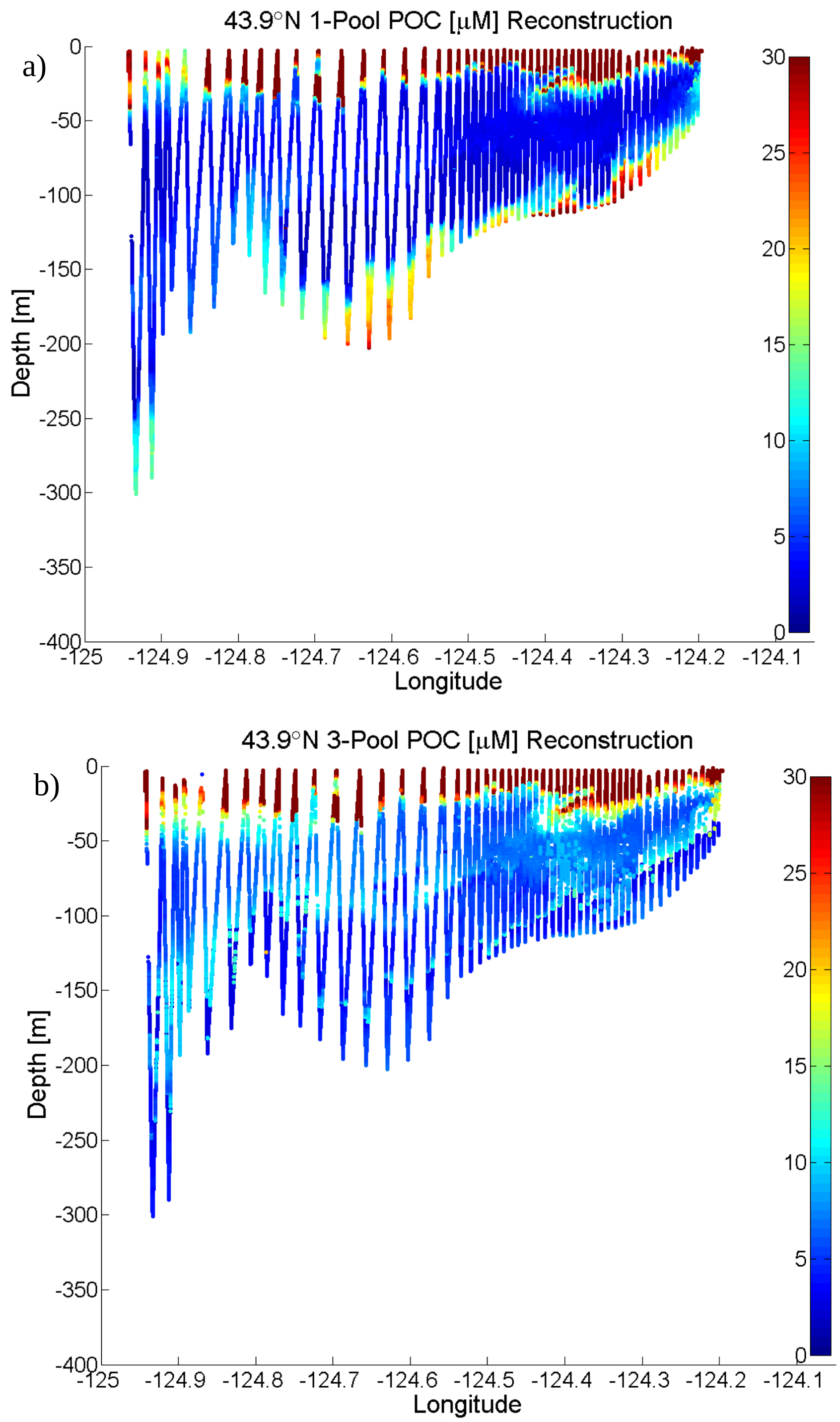

Figure 18 – a) A derivation of water column POC concentrations using three POC-c_p calibrations which correspond to particle pools distinguished by varying optical ratios. b) A derivation of water column POC using a simple one particle pool c_p calibration on the same measurements.

The significance of the differences between the two forms of derivation is clearly illustrated using the three particle pools to derive a POC inventory (g C) for each area of the water column (Table 4). These inventories were calculated by assuming that the volume of water within the 43.9ºN transect (at 1m width) is approximately 9.0×10^6 m^3 and by assuming that the BBL, mid-water, and surface pools constitute ~20%, ~55%, and ~25% of the total water volume respectively. The POC of the BBL as found using three particle pools is less than 1/3 of that of the same water mass derived using one particle pool. Conversely, in the case of the mid-water, the POC inventory calculated using the three-pool approach is 3 times higher than with the one-pool approach. The POC inventory of the surface does not change significantly from one method of derivation to the other. These results show that the distribution of POC within the water column during the May cruise differs significantly from the distribution implied by a simple linear relationship between POC and optical beam attenuation.

	1 Particle Pool	3 Particle Pools
BBL	2.5×10^5 g C	7.0×10^4 g C
MID	1.3×10^5 g C	3.9×10^5 g C
TOP	1.1×10^6 g C	1.1×10^6 g C

Table 4 – POC standing stock of the water column divided between three particle areas. Carbon content derived first using the single particle pool c_p relationship, second using the three pool relationship.

5. Conclusions

We developed a filtration system (SAFS) that allows us to sample particulate organic carbon at a higher resolution than was previously possible. SAFS collects particulate samples on 13mm GF filters from a continuously flowing water stream at user-designated time intervals. Testing performed during the summer of 2008 shows that SAFS collects samples that are comparable to samples collected by manual filtration, but does so more efficiently. This allows us to collect discrete samples at a high enough resolution to capture gradients in water masses that otherwise would only be seen in optical measurements. Furthermore, the variability seen within the POC samples corresponds to the physical and optical properties of changing water masses.

SAFS was deployed during the summer of 2009 alongside a suite of other chemical and optical measurements in order to better constrain the dynamics of carbon cycling within the coastal Oregon upwelling system. By combining POC samples with optical measurements, we find that three distinct particle pools can be discerned within the water column, corresponding with photo-productive surface waters, varied sub-surface waters, and dense bottom boundary layer water. Through the use of optical ratios, it is possible to segregate these three particle pools and determine POC-c_p calibrations for each pool, enabling us to derive a more accurate distribution of POC from *in situ* optical measurements. From this new distribution (Figure 18), we find a decoupling of sediment and carbon in the bottom boundary layer, and a previously undetected relative elevation in mid-water POC. Both of these features have implications for quantifying carbon content and for understanding transport dynamics.

References

Bakun, A. (1990). "Global Climate Change and Intensification of Coastal Ocean Upwelling." Science **247**(4939): 198-201.

Bandstra, L., B. Hales, et al. (2006). "High-frequency measurements of total CO2: Method development and first oceanographic observations." Marine Chemistry **100**(1-2): 24-38.

Bane, J. M., M. D. Levine, et al. (2005). "Atmospheric forcing of the Oregon coastal ocean during the 2001 upwelling season." Journal of Geophysical Research-Oceans **110**(C10).

Behrenfeld, M. J. and E. Boss (2003). "The beam attenuation to chlorophyll ratio: an optical index of phytoplankton physiology in the surface ocean?" Deep-Sea Research Part I-Oceanographic Research Papers **50**(12): 1537-1549.

Behrenfeld, M. J. and E. Boss (2006). "Beam attenuation and chlorophyll concentration as alternative optical indices of phytoplankton biomass." Journal of Marine Research **64**(3): 431-451.

Behrenfeld, M. J., E. Boss, et al. (2005). "Carbon-based ocean productivity and phytoplankton physiology from space." Global Biogeochemical Cycles **19**(1).

Benthien, A., I. Zondervan, et al. (2007). "Carbon isotopic fractionation during a mesocosm bloom experiment dominated by Emiliania huxleyi: Effects of CO2 concentration and primary production." Geochimica Et Cosmochimica Acta **71**(6): 1528-1541.

Boss, E., W. S. Pegau, et al. (2001). "Spectral particulate attenuation and particle size distribution in the bottom boundary layer of a continental shelf." Journal of Geophysical Research-Oceans **106**(C5): 9509-9516.

Boss, E., W. S. Pegau, et al. (2004). "Particulate backscattering ratio at LEO 15 and its use to study particle composition and distribution." Journal of Geophysical Research-Oceans **109**(C1).

Boss, E., W. S. Pegau, et al. (2001). "Spatial and temporal variability of absorption by dissolved material at a continental shelf." Journal of Geophysical Research-Oceans **106**(C5): 9499-9507.

Boss, E., L. Taylor, et al. (2009). "Comparison of inherent optical properties as a surrogate for particulate matter concentration in coastal waters." Limnology and Oceanography-Methods **7**: 803-810.

Chase, Z., A. van Geen, et al. (2002). "Iron, nutrient, and phytoplankton distributions in Oregon coastal waters." Journal of Geophysical Research-Oceans **107**(C10).

Chavez, F. P. and J. R. Toggweiler (1995). Physical estimates of global new production: the upwelling contribution. Upwelling in the Ocean: Modern Processes and Ancient Records. E. P. Summerhayes, K. C. Emis, M. V. Angel, R. L. Smith and B. Zeitzschel. Chichester, John Wiley & Sons**:** 313-320.

Dickson, M.-L. and P. A. Wheeler (1995). "NitrateUptake Rates in a Coastal Upwelling Regime: A Comparison of PN-Specific, Absolute, and Chl a-Specific Rates." Limnology and Oceanography **40**(3): 533-543.

Dugdale, R. C., F. P. Wilkerson, et al. (1990). "Realization of new production in coastal upwelling areas - a means to compare relative performance." Limnology and Oceanography **35**(4): 822-829.

Eisner, L. B. and T. J. Cowles (2005). "Spatial variations in phytoplankton pigment ratios, optical properties, and environmental gradients in Oregon coast surface waters." J. Geophys. Res. **110**.

Fennel, K. and E. Boss (2003). "Subsurface Maxima of Phytoplankton and Chlorophyll: Steady-State Solutions from a Simple Model." Limnology and Oceanography **48**(4): 1521-1534.

Gardner, W. D., J. C. Blakey, et al. (2001). "Optics, particles, stratification, and storms on the New England continental shelf." J. Geophys. Res. **106**(C5): 9473-9497.

Gardner, W. D., M. J. Richardson, et al. (2003). "Determining true particulate organic carbon: bottles, pumps and methodologies." Deep-Sea Research Part Ii-Topical Studies in Oceanography **50**(3-4): 655-674.

Goñi, M. A., H. L. Aceves, et al. (2003). "Biogenic fluxes in the Cariaco Basin: a combined study of sinking particulates and underlying sediments." Deep Sea Research Part I: Oceanographic Research Papers **50**(6): 781-807.

Goni, M. A., M. W. Cathey, et al. (2005). "Fluxes and sources of suspended organic matter in an estuarine turbidity maximum region during low discharge conditions." Estuarine Coastal and Shelf Science **63**(4): 683-700.

Goni, M. A., N. Monacci, et al. (2006). "Distribution and sources of particulate organic matter in the water column and sediments of the Fly River Delta, Gulf of Papua (Papua New Guinea)." Estuarine Coastal and Shelf Science **69**(1-2): 225-245.

Goni, M. A., M. J. Teixeira, et al. (2003). "Sources and distribution of organic matter in a river-dominated estuary (Winyah Bay, SC, USA)." Estuarine Coastal and Shelf Science **57**(5-6): 1023-1048.

Hales, B., L. Karp-Boss, et al. (2006). "Oxygen production and carbon sequestration in an upwelling coastal margin." Global Biogeochemical Cycles **20**(3): -.

Hales, B. and T. Takahashi (2002). "The pumping SeaSoar: A high-resolution seawater sampling platform." Journal of Atmospheric and Oceanic Technology **19**(7): 1096-1104.

Hales, B., T. Takahashi, et al. (2005). "Atmospheric CO_2 uptake by a coastal upwelling system." Global Biogeochemical Cycles **19**(1): -.

Hales, B., R. D. Vaillancourt, et al. (2009). "High-resolution surveys of the biogeochemistry of the New England shelfbreak front during Summer, 2002." Journal of Marine Systems **78**(3): 426-441.

Hill, J. K. and P. A. Wheeler (2002). "Organic carbon and nitrogen in the northern California current system: comparison of offshore, river plume, and coastally upwelled waters." Progress in Oceanography **53**(2-4): 369-387.

Karp-Boss, L., P. A. Wheeler, et al. (2004). "Distributions and variability of particulate organic matter in a coastal upwelling system." Journal of Geophysical Research-Oceans **109**(C9): -.

Kudela, R. M., N. Garfield, et al. (2006). "Bio-optical signatures and biogeochemistry from intense upwelling and relaxation in coastal California." Deep-Sea Research Part Ii-Topical Studies in Oceanography **53**(25-26): 2999-3022.

Laws, E. A., et al. (2002). 13C discrimination patterns in oceanic phytoplankton: likely influence of CO2 concentrating mechanisms, and implications for palaeoreconstructions. Collingwood, AUSTRALIE, Commonwealth Scientific and Industrial Research Organization.

Laws, E. A., R. R. Bidigare, et al. (1997). "Effect of Growth Rate and CO2 Concentration on Carbon Isotopic Fractionation by the Marine Diatom Phaeodactylum tricornutum." Limnology and Oceanography **42**(7): 1552-1560.

Lentz, S. J. and J. H. Trowbridge (1991). "The Bottom Boundary Layer Over the Northern California Shelf." Journal of Physical Oceanography **21**(8): 1186-1201.

Loder, T. C. and D. W. Hood (1972). "Distribution of Organic Carbon in a Glacial Estuary in Alaska." Limnology and Oceanography **17**(3): 349-355.

Loisel, H., X. Meriaux, et al. (2007). "Investigation of the optical backscattering to scattering ratio of marine particles in relation to their biogeochemical composition in the eastern English Channel and southern North Sea." Limnology and Oceanography **52**(2): 739-752.

Loubere, P., S. A. Siedlecki, et al. (2007). "Organic carbon and carbonate fluxes: Links to climate change." Deep-Sea Research Part Ii-Topical Studies in Oceanography **54**(5-7): 437-446.

Moran, S. B., M. A. Charette, et al. (1999). "Differences in seawater particulate organic carbon concentration in samples collected using small- and large-volume methods: the importance of DOC adsorption to the filter blank." Marine Chemistry **67**(1-2): 33-42.

Muller-Karger, F. E., R. Varela, et al. (2005). "The importance of continental margins in the global carbon cycle." Geophysical Research Letters **32**(1).

Perlin, A., J. N. Moum, et al. (2005). "Response of the bottom boundary layer over a sloping shelf to variations in alongshore wind." Journal of Geophysical Research-Oceans **110**(C10).

Prieto, L., R. D. Vaillancourt, et al. (2008). "On the relationship between carbon fixation efficiency and bio-optical characteristics of phytoplankton." Journal of Plankton Research **30**(1): 43-56.

Riebesell, U., S. Burkhardt, et al. (2000). "Carbon isotope fractionation by a marine diatom: dependence on the growth-rate-limiting resource." Marine Ecology-Progress Series **193**: 295-303.

Small, L. F. and D. W. Menzies (1981). "Patterns of primary productivity and biomass in a coastal upwelling region." Journal Name: Deep-Sea Res., Part A; (United Kingdom); Journal Volume: 28A: Medium: X; Size: Pages: 123-149.

Snyder, W. A., R. A. Arnone, et al. (2008). "Optical scattering and backscattering by organic and inorganic particulates in U.S. coastal waters." Appl. Opt. **47**(5): 666-677.

Thunell, R., C. Benitez-Nelson, et al. (2007). "Particulate organic carbon fluxes along upwelling-dominated continental margins: Rates and mechanisms." Global Biogeochemical Cycles **21**(1).

Trowbridge, J. H. and S. J. Lentz (1998). "Dynamics of the bottom boundary layer on the northern California shelf." Journal of Physical Oceanography **28**(10): 2075-2093.

Wetz, M. S., B. Hales, et al. (2009). "Degradation of phytoplankton-derived organic matter: Implications for carbon and nitrogen biogeochemistry in coastal ecosystems (vol 77, pg 422, 2008)." Estuarine Coastal and Shelf Science **83**(4): 659-659.

Wetz, M. S. and P. A. Wheeler (2003). "Production and Partitioning of Organic Matter during Simulated Phytplankton Blooms." Limnology and Oceanography **48**(5): 1808-1817.

Wetz, M. S. and P. A. Wheeler (2004). "Response of bacteria to simulated upwelling phytoplankton blooms." Marine Ecology-Progress Series **272**: 49-57.

Wetz, M. S. and P. A. Wheeler (2007). "Release of dissolved organic matter by coastal diatoms." Limnology and Oceanography **52**(2): 798-807.

Whitmire, A. L., E. Boss, et al. (2007). "Spectral variability of the particulate backscattering ratio." Optics Express **15**(11): 7019-7031.

Woodworth, M., M. Goni, et al. (2004). "Oceanographic controls on the carbon isotopic compositions of sinking particles from the Cariaco Basin." Deep-Sea Research Part I-Oceanographic Research Papers **51**(12): 1955-1974.

APPENDICES

Appendix A

Figure A1 - Image of the semi-automated filtration system mounted on the lab bench in R/V Wecoma's wet lab.

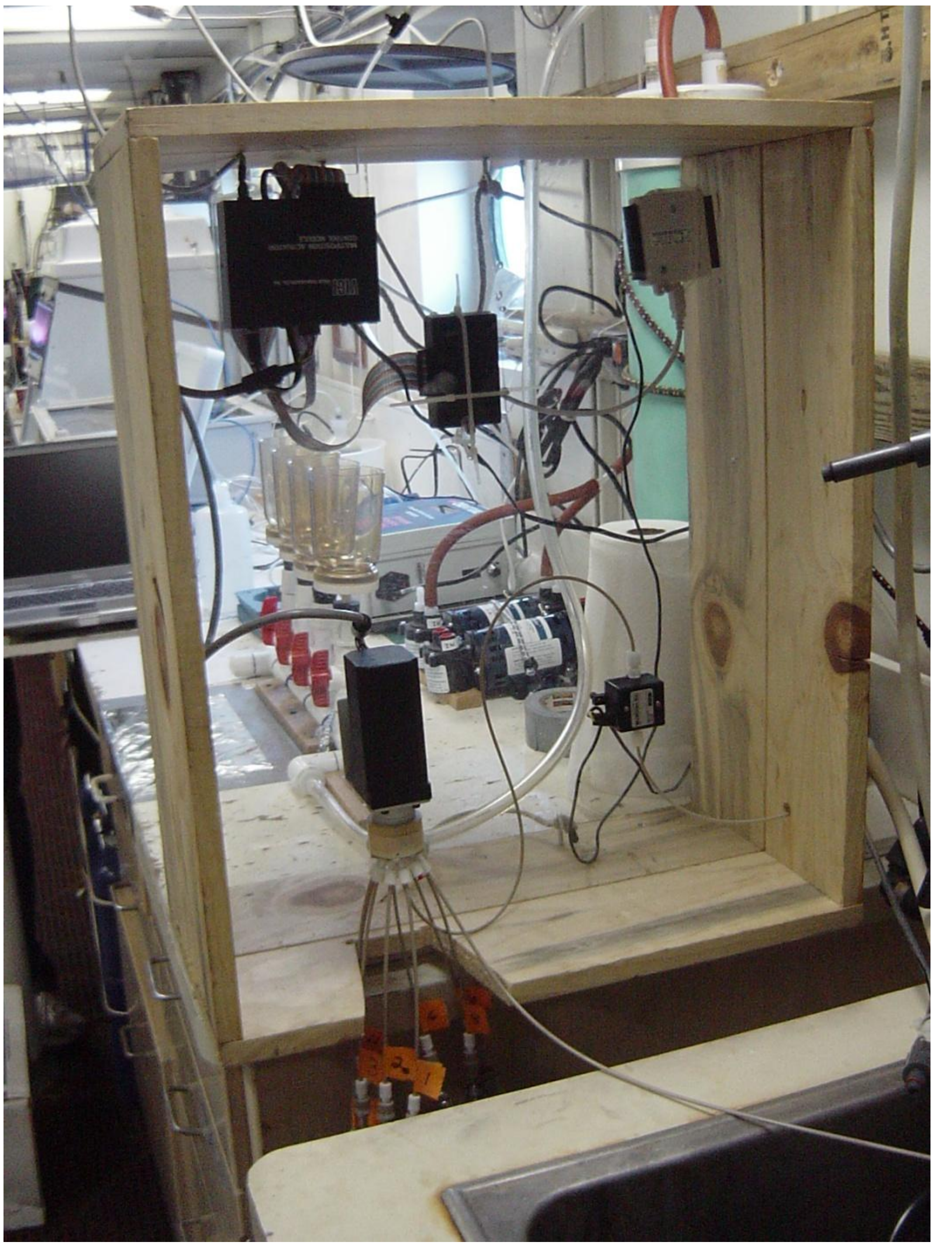

Figure A2 - Image of the user interface for the LabView software controlling the semi-automated filtration system.

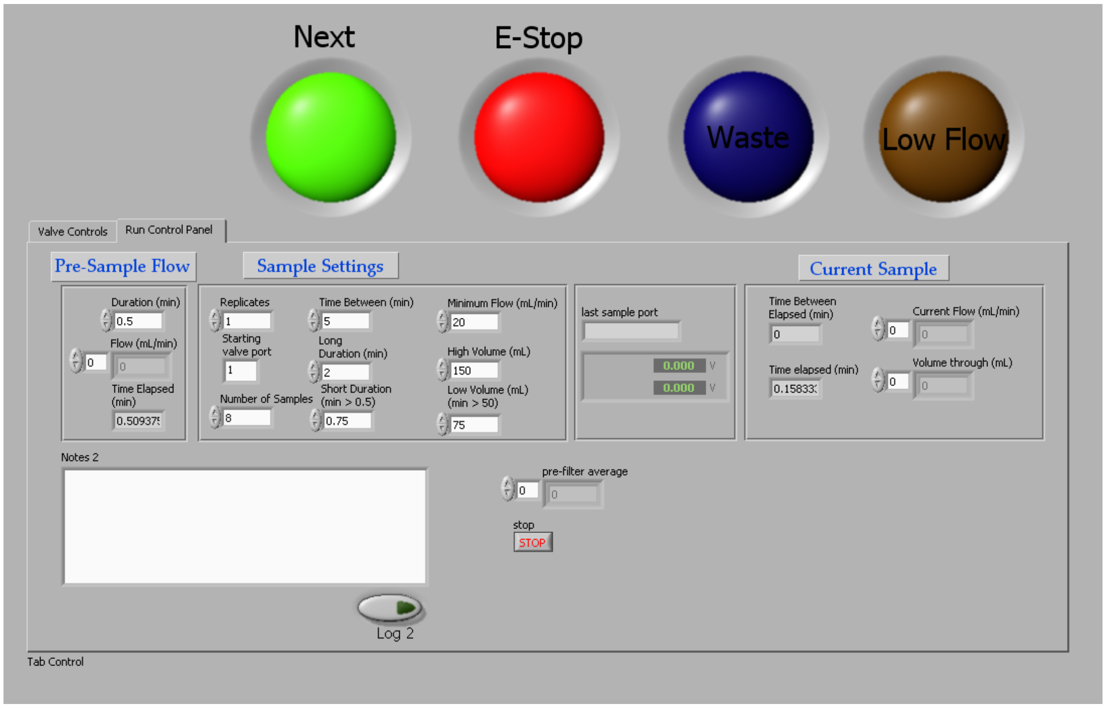

Table A1 – Example of data output recorded by LabView software. Output includes flow rate (mL/min), raw flow data (V), filter number, total volume (mL), date/time, and Julian Day.

80.442214	3.668966	1	0.670352	5/31/2005 00:05	152.004058
80.769689	3.684262	1	1.343433	5/31/2005 00:05	152.004059
81.370058	3.712307	1	2.021516	5/31/2005 00:05	152.004064
80.605952	3.676614	1	2.693233	5/31/2005 00:05	152.00407
80.551373	3.674064	1	3.364494	5/31/2005 00:05	152.004076
80.278477	3.661317	1	4.033481	5/31/2005 00:05	152.004082
80.387635	3.666416	1	4.703378	5/31/2005 00:05	152.004088
80.442214	3.668966	1	5.37373	5/31/2005 00:05	152.004093
80.605952	3.676614	1	6.045446	5/31/2005 00:05	152.004099
81.097163	3.699559	1	6.721256	5/31/2005 00:05	152.004105
80.824268	3.686812	1	7.394792	5/31/2005 00:05	152.004111
81.370058	3.712307	1	8.072875	5/31/2005 00:05	152.004116
80.988005	3.69446	1	8.747775	5/31/2005 00:05	152.004122
81.206321	3.704658	1	9.424495	5/31/2005 00:05	152.004128
81.097163	3.699559	1	10.100305	5/31/2005 00:05	152.004134
80.988005	3.69446	1	10.775205	5/31/2005 00:05	152.00414
80.605952	3.676614	1	11.446921	5/31/2005 00:05	152.004145
79.787266	3.638372	1	12.111815	5/31/2005 00:05	152.004151
79.623529	3.630723	1	12.775344	5/31/2005 00:05	152.004157
79.241475	3.612877	1	13.43569	5/31/2005 00:05	152.004163
79.241475	3.612877	1	14.096035	5/31/2005 00:06	152.004169
79.623529	3.630723	1	14.759565	5/31/2005 00:06	152.004174
79.56895	3.628174	1	15.422639	5/31/2005 00:06	152.00418
79.732687	3.635822	1	16.087078	5/31/2005 00:06	152.004186
80.005582	3.64857	1	16.753792	5/31/2005 00:06	152.004192
80.769689	3.684262	1	17.426872	5/31/2005 00:06	152.004197
80.824268	3.686812	1	18.100408	5/31/2005 00:06	152.004203
80.933426	3.691911	1	18.774853	5/31/2005 00:06	152.004209
80.824268	3.686812	1	19.448389	5/31/2005 00:06	152.004215
80.387635	3.666416	1	20.118286	5/31/2005 00:06	152.004221
80.223898	3.658768	1	20.786818	5/31/2005 00:06	152.004226
79.678108	3.633273	1	21.450802	5/31/2005 00:06	152.004232
79.623529	3.630723	1	22.114332	5/31/2005 00:06	152.004238
79.241475	3.612877	1	22.774677	5/31/2005 00:06	152.004244
79.296054	3.615427	1	23.435478	5/31/2005 00:06	152.00425
79.459791	3.623075	1	24.097643	5/31/2005 00:06	152.004255
79.023159	3.602679	1	24.756169	5/31/2005 00:06	152.004261
79.186896	3.610328	1	25.41606	5/31/2005 00:06	152.004267

Appendix B

Table B1. - Table and plot of results of July 2008 in-lab comparison of manual vs. automatic filtration methods.

	n	POC (µM)	Standard Error	% Error	n	POC (µM)	Standard Error	% Error
Surface	Manual Filtration				Auto Filtration			
LB15	3	55.013	0.362	0.007	3	49.665	0.087	0.002
LB30	3	19.764	1.309	0.066	3	18.576	1.711	0.092
LB50	3	19.514	1.049	0.054	3	18.848	1.360	0.072
LB70	3	21.755	3.658	0.168	3	13.617	0.554	0.041
LB100	3	10.051	0.603	0.060	3	8.144	0.305	0.037
NH1	3	14.525	1.584	0.109	3	11.239	1.171	0.104
NH3	3	9.366	0.565	0.060	3	8.535	0.203	0.024
NH5	3	8.940	1.267	0.142	3	4.331	0.229	0.053
NH10	3	12.770	1.010	0.079	3	11.334	0.300	0.026
Near-bottom								
LB15	2	21.268	2.938	0.138	3	25.659	4.532	0.177
LB30	3	21.270	3.381	0.159	3	20.469	2.538	0.124
LB50	2	14.768	1.099	0.074	3	13.513	0.392	0.029
LB70	3	11.741	0.273	0.023	2	8.879	0.357	0.040
LB100	3	13.695	1.200	0.088	3	10.915	0.928	0.085
NH1	2	13.129	0.422	0.032	3	6.856	0.563	0.082
NH3	2	13.352	2.589	0.194	3	8.827	0.834	0.094
NH5	2	10.873	0.904	0.083	3	6.100	0.577	0.095
NH10	3	12.965	1.917	0.148	3	9.458	0.465	0.049

Table B2. - A table and plots of the manual/automatic comparison results from W0809A

	POC (mg/L)	
	Manual	Automatic
	13.994	12.555
	13.761	12.702
	17.024	12.876
	14.409	14.553
	14.540	15.612
	13.934	18.644
	14.873	
	15.865	
Mean	14.800	14.490
Standard Error	0.396	0.967
% Error	2.68%	6.68%

Figure B1. – Bar and whisker plot of the manual/automatic comparison results from W0809A.

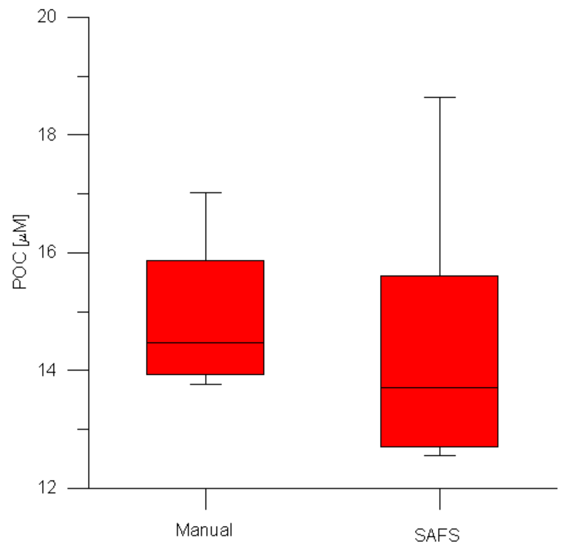

Table B.3. –Table of results from the Sept. 10, 2008 under way sampling.

Date/Time	Latitude	Longitude	OC µM	N µM	(OC:N)a	Fluor [V]	c_p	Salinity [PSU]	Temp [ºC]
9/10/08 3:19	45.326	-124.230	82.06	11.14	7.4	1.27	2.58	32.12	12.11
9/10/08 3:29	45.327	-124.233	80.53	11.65	6.9	1.18	2.08	32.10	12.27
9/10/08 3:39	45.310	-124.242	70.44	10.09	7.0	1.19	1.86	32.16	11.79
9/10/08 3:49	45.293	-124.253	58.28	8.35	7.0	1.07	1.60	32.27	11.74
9/10/08 3:59	45.277	-124.264	41.60	6.12	6.8	0.86	1.50	32.11	12.29
9/10/08 4:09	45.261	-124.274	46.82	7.85	6.0	1.01	1.55	32.09	12.33
9/10/08 4:19	45.244	-124.285	35.93	5.64	6.4	0.76	1.40	32.02	13.18
9/10/08 4:29	45.228	-124.296	19.97	3.66	5.5	0.49	1.12	31.90	13.53
9/10/08 4:39	45.212	-124.306	15.25	2.70	5.7	0.39	1.00	31.86	13.99
9/10/08 4:49	45.195	-124.317	23.38	4.61	5.1	0.33	0.81	31.74	14.31
9/10/08 4:59	45.179	-124.327	12.37	1.96	6.3	0.27	0.95	31.62	14.81
9/10/08 5:09	45.163	-124.338	10.55	2.40	4.4	0.27	0.81	31.58	14.88
9/10/08 5:19	45.147	-124.349	15.96	2.40	6.6	0.25	0.80	31.52	14.90
9/10/08 5:30	45.128	-124.361	12.42	2.74	4.5	0.27	0.81	31.51	14.77
9/10/08 5:40	45.111	-124.371	12.15	1.91	6.4	0.31	0.82	31.61	14.63
9/10/08 5:50	45.094	-124.383	12.46	2.81	4.4	0.32	0.84	31.64	14.63
9/10/08 6:04	45.070	-124.398	12.65	2.03	6.2	0.29	0.81	31.64	14.81
9/10/08 6:14	45.054	-124.408	10.29	2.54	4.0	0.26	0.75	31.60	15.00
9/10/08 6:24	45.037	-124.419	13.21	2.20	6.0	0.27	0.76	31.57	15.01
9/10/08 6:34	45.021	-124.430	15.67	2.79	5.6	0.27	0.76	31.64	15.02
9/10/08 6:45	45.003	-124.441	16.97	2.26	7.5	0.27	0.75	31.69	15.03
9/10/08 6:54	44.989	-124.450	16.52	2.82	5.9	0.26	0.75	31.73	15.04
9/10/08 7:05	44.971	-124.461	17.14	2.49	6.9	0.29	0.76	31.72	15.03
9/10/08 7:15	44.954	-124.472	15.23	2.75	5.5	0.28	0.74	31.73	15.07
9/10/08 7:25	44.938	-124.482	12.50	2.33	5.4	0.22	0.65	31.89	15.25
9/10/08 7:36	44.920	-124.495	11.91	1.59	7.5	0.17	0.58	31.98	15.42
9/10/08 7:45	44.905	-124.502	12.47	2.10	5.9	0.18	0.58	32.07	15.32
9/10/08 7:55	44.904	-124.503	12.55	2.11	5.9	0.19	0.58	32.09	15.30
9/10/08 8:05	44.904	-124.503	20.85	3.56	5.9	0.19	0.57	32.08	15.32
9/10/08 8:16	44.904	-124.503	13.95	2.22	6.3	0.18	0.56	32.08	15.32
9/10/08 8:25	44.903	-124.502	14.71	2.69	5.5	0.18	0.57	32.08	15.31
9/10/08 8:35	44.891	-124.501	10.73	2.09	5.1	0.19	0.56	32.09	15.31
9/10/08 8:45	44.875	-124.497	9.86	1.69	5.8	0.15	0.54	32.01	15.42
9/10/08 8:55	44.859	-124.494	11.28	1.90	5.9	0.15	0.56	31.91	15.24
9/10/08 9:07	44.849	-124.482	10.36	1.86	5.6	0.21	0.60	31.73	14.93
9/10/08 9:17	44.850	-124.462	10.44	2.10	5.0	0.23	0.62	31.64	14.87
9/10/08 9:37	44.849	-124.417	13.58	2.39	5.7	0.31	0.73	31.84	14.04
9/10/08 9:47	44.849	-124.394	14.47	2.42	6.0	0.40	0.78	31.95	14.10
9/10/08 9:57	44.849	-124.372	13.10	2.23	5.9	0.33	0.74	32.00	13.40
9/10/08 10:08	44.849	-124.347	16.68	2.75	6.1	0.48	0.82	32.09	12.71
9/10/08 10:18	44.849	-124.325	13.86	2.49	5.6	0.42	0.70	32.11	12.67
9/10/08 10:28	44.849	-124.303	14.07	2.27	6.2	0.38	0.65	32.11	12.75
9/10/08 10:38	44.849	-124.280	12.77	2.26	5.7	0.34	0.61	32.13	12.46
9/10/08 10:48	44.849	-124.257	12.30	2.11	5.8	0.30	0.58	32.16	12.04
9/10/08 10:58	44.849	-124.234	14.36	2.66	5.4	0.37	0.63	32.27	10.85

Table B.3. (continued)

Date/Time	Latitude	Longitude	OC µM	N µM	(OC:N)a	Fluor [V]	c_p	Salinity [PSU]	Temp [ºC]
9/10/08 11:08	44.849	-124.212	21.01	3.63	5.8	0.45	0.71	32.47	10.24
9/10/08 11:18	44.849	-124.189	17.61	3.06	5.8	0.35	0.61	32.53	9.91
9/10/08 11:31	44.850	-124.159	31.64	5.59	5.7	0.66	0.88	32.83	9.47
9/10/08 11:41	44.850	-124.135	40.19	6.83	5.9	0.82	1.01	32.91	9.03
9/10/08 11:51	44.849	-124.111	23.19	4.16	5.6	0.45	0.69	33.00	8.39
9/10/08 12:21	44.814	-124.115	10.70	2.04	5.2	0.12	0.63	33.75	8.65
9/10/08 12:31	44.781	-124.118	24.93	4.35	5.7	0.11	0.70	33.76	9.17
9/10/08 12:41	44.747	-124.120	37.61	6.45	5.8	0.77	1.15	33.62	8.90

Appendix C

Figure C.1. – Cross-sections of both the 45º and 43.9ºN transect depicting the smearing of each POC sample.

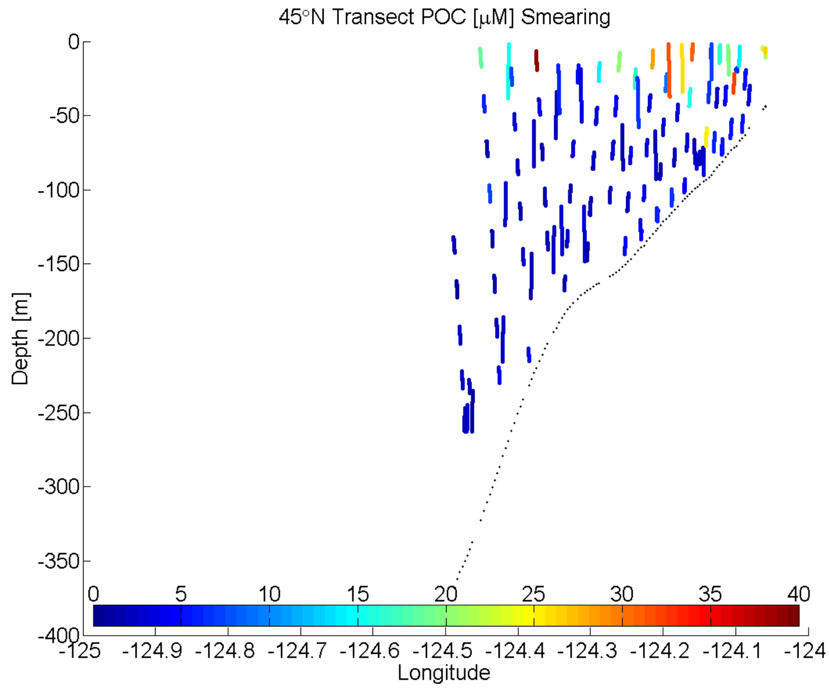

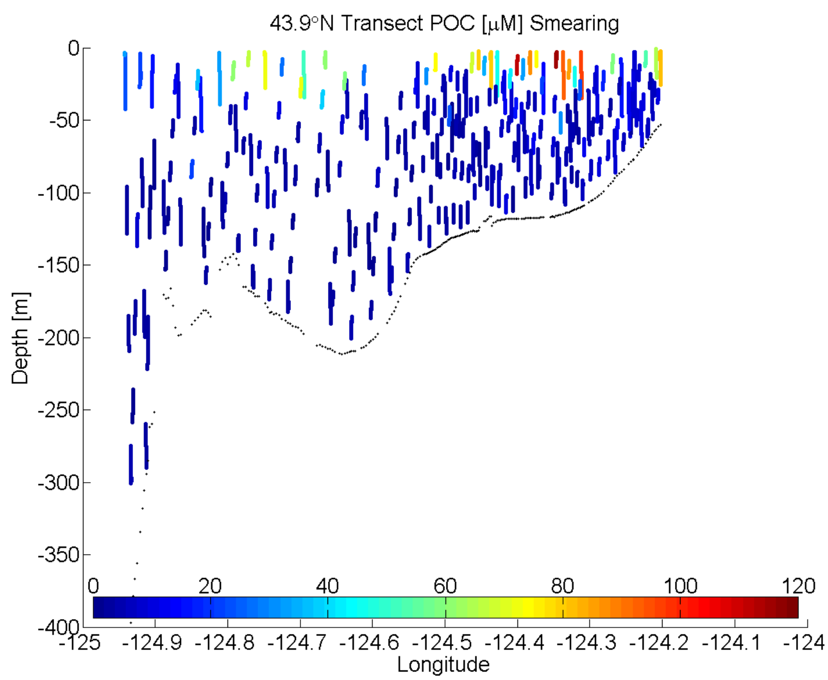

Figure C2. – Plots of POC concentrations within both transects with a forced color scale to show low-concentration variability within each cross-section.

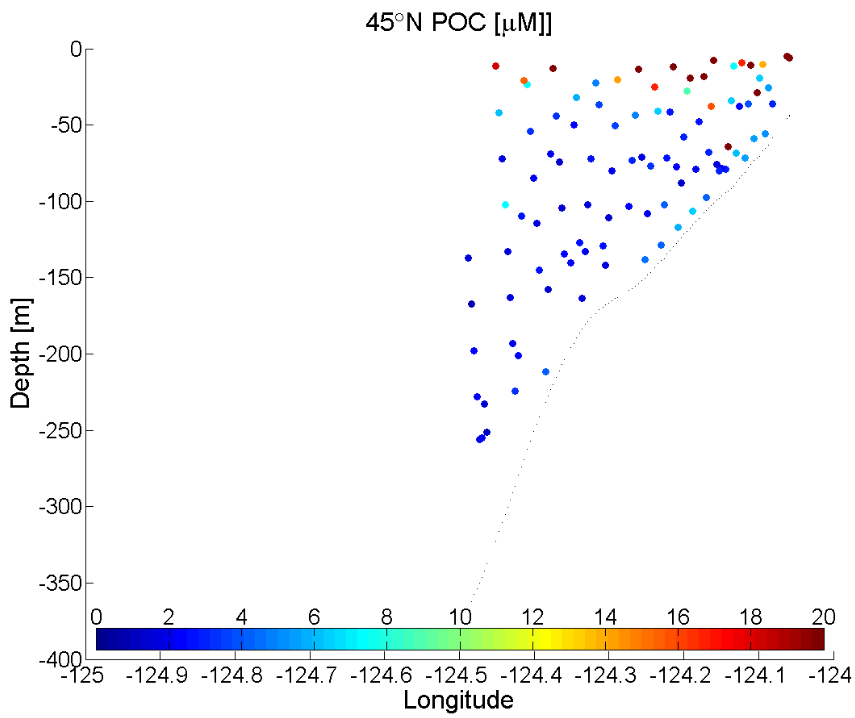

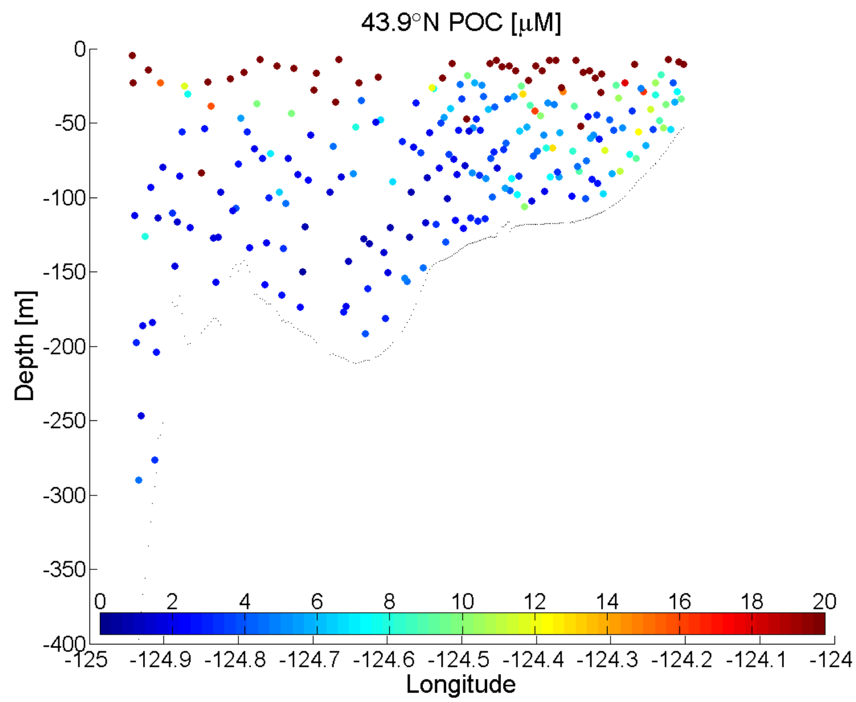

Figure C3. – Cross-sections of high-resolution temperature and salinity measurements from both 45º and 44ºN overlaid with contours of constant density.

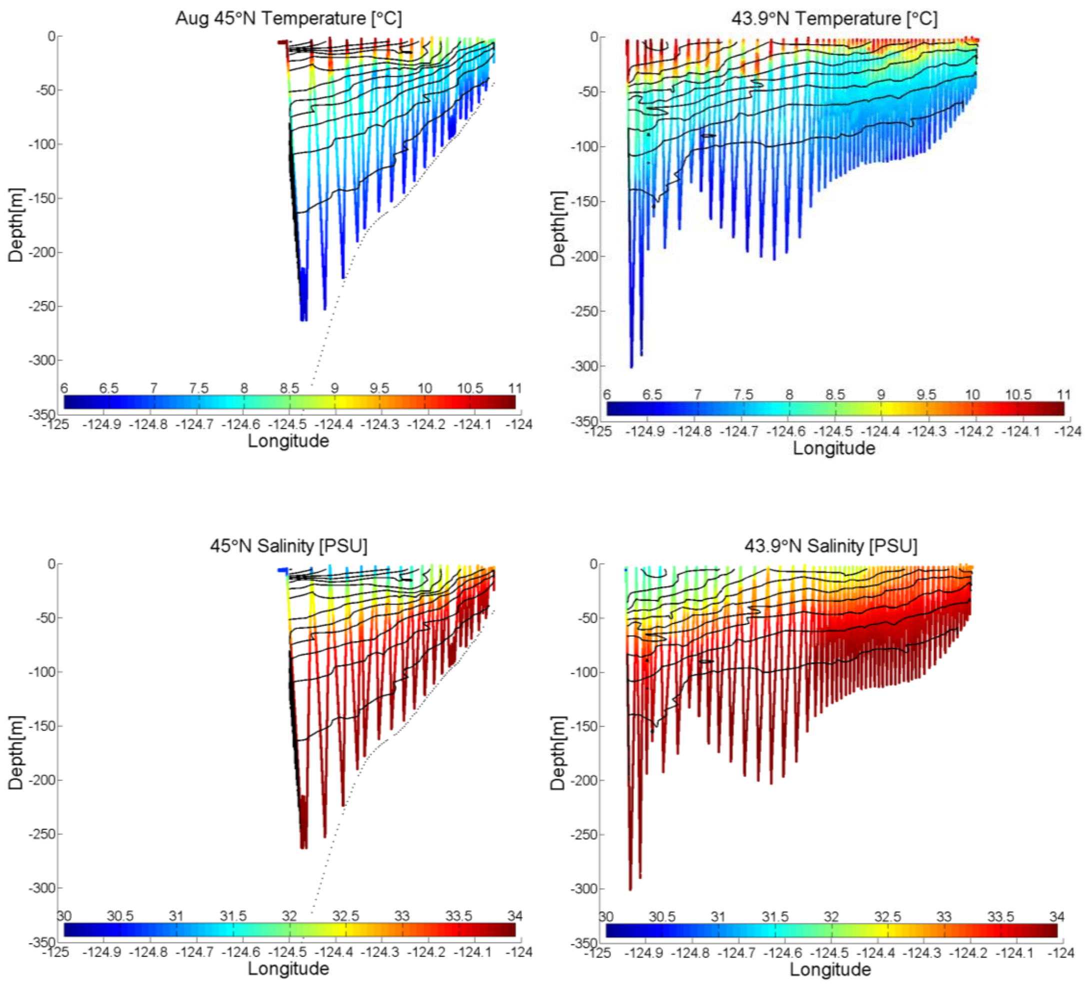

Figure C4. – Cross-section plots of POC resolution optical ratios.

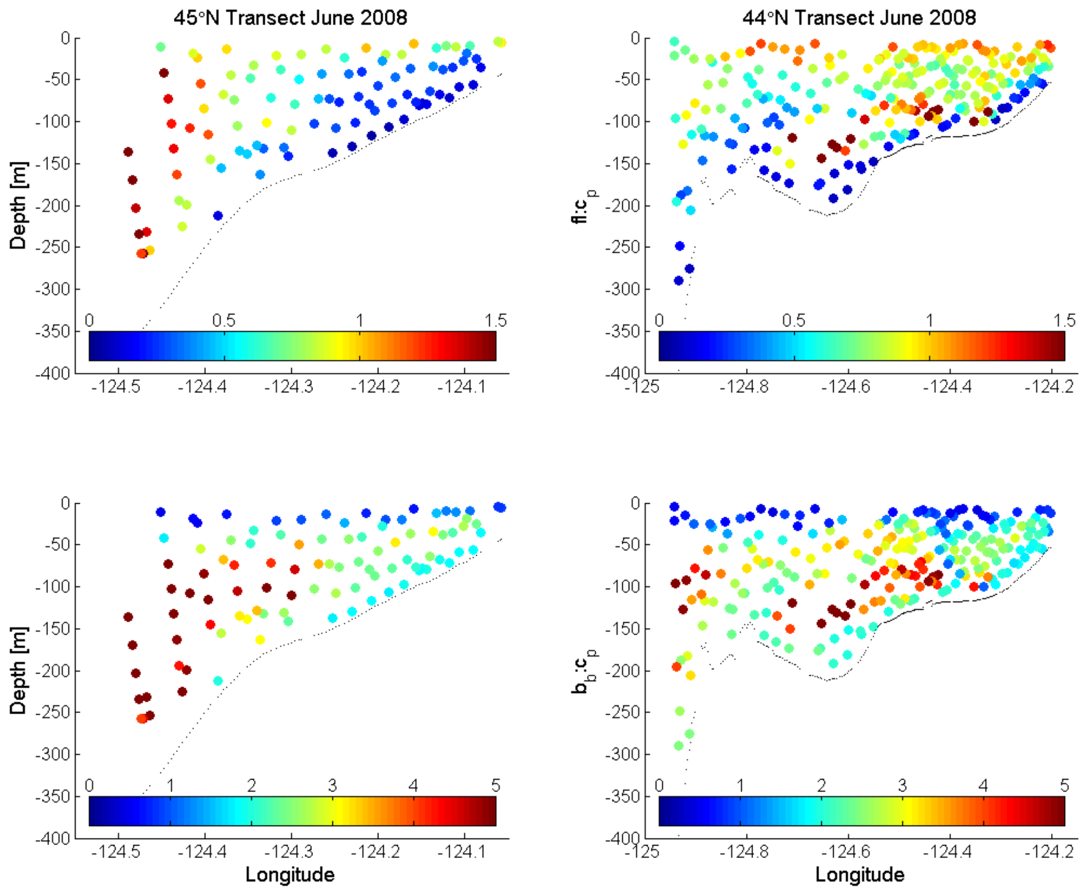

Table C1. – Raw POC data from W0905B transects at 45ºN and 43.9ºN. Relevant in situ measurements are included. The solid line on page 60 indicates the transition from 45ºN to 43.9ºN data.

POC Start time	POC End time	OC [µM]	Insitu Time	Lat	Long	Ship Depth [m]	Fish Depth [m]	T [ºC]	S [PSU]	Backscatter [V]	Transmissometery [V]	O2 [V]	Chlorophyll Fluorescence [v]	Cp [m^{-1}]
150.647	150.648	26.696	150.648	45.008	-124.059	43.653	6.097	8.159	33.089	0.074	4.008	1.622	0.799	0.530
150.651	150.652	21.681	150.651	45.008	-124.059	43.919	5.961	8.299	33.034	0.083	3.906	2.875	0.896	0.632
150.654	150.656	22.836	150.655	45.009	-124.062	45.782	4.823	8.245	33.013	0.075	3.942	2.622	0.784	0.595
150.672	150.673	2.945	150.672	45.007	-124.081	58.569	36.242	7.278	33.779	0.061	4.365	1.657	0.201	0.186
150.677	150.678	5.539	150.677	45.006	-124.087	63.182	25.873	7.601	33.596	0.050	4.448	2.162	0.195	0.111
150.680	150.681	5.059	150.681	45.006	-124.091	65.491	55.917	6.704	33.902	0.079	4.274	1.532	0.206	0.270
150.684	150.685	13.841	150.684	45.005	-124.095	67.007	10.421	8.081	32.923	0.061	4.159	2.596	0.618	0.395
150.687	150.688	6.356	150.688	45.005	-124.099	70.715	19.156	7.724	33.297	0.044	4.482	2.944	0.198	0.081
150.691	150.692	32.179	150.691	45.004	-124.102	71.800	28.580	7.625	33.542	0.044	4.486	2.150	0.192	0.077
150.694	150.695	5.537	150.695	45.004	-124.106	73.338	58.937	6.726	33.900	0.069	4.321	1.518	0.199	0.227
150.698	150.699	19.879	150.698	45.003	-124.110	76.058	10.761	8.197	32.767	0.068	4.049	1.237	0.797	0.497
150.701	150.702	4.009	150.702	45.003	-124.114	77.860	36.038	7.394	33.729	0.047	4.452	1.896	0.194	0.107
150.705	150.707	5.336	150.706	45.002	-124.118	81.226	71.498	6.648	33.912	0.085	4.244	1.428	0.204	0.298
150.709	150.710	16.653	150.709	45.001	-124.122	82.996	9.040	8.126	32.633	0.054	4.207	1.546	0.532	0.340
150.712	150.714	2.333	150.713	45.001	-124.126	85.022	37.962	7.544	33.646	0.044	4.474	2.088	0.193	0.088
150.716	150.717	6.009	150.716	45.000	-124.130	87.498	68.500	6.729	33.900	0.066	4.340	1.597	0.196	0.210
150.719	150.721	7.392	150.720	45.000	-124.133	90.024	11.403	8.107	32.704	0.053	4.249	1.600	0.462	0.299
150.723	150.724	6.436	150.723	45.000	-124.137	91.549	34.315	7.658	33.512	0.041	4.508	2.384	0.192	0.058
150.726	150.727	25.039	150.727	45.000	-124.140	93.098	64.235	7.053	33.835	0.044	4.481	1.956	0.191	0.081
150.730	150.731	3.054	150.730	45.000	-124.144	94.497	79.038	6.701	33.902	0.064	4.356	1.579	0.195	0.195
150.735	150.736	2.292	150.735	45.000	-124.149	96.440	78.553	6.776	33.891	0.061	4.357	1.539	0.193	0.194
150.738	150.739	2.822	150.739	45.000	-124.153	97.864	80.311	6.699	33.901	0.060	4.364	1.568	0.194	0.187
150.742	150.743	1.686	150.742	45.000	-124.156	99.302	75.871	6.896	33.863	0.046	4.451	1.583	0.192	0.108
150.745	150.746	30.993	150.746	45.000	-124.160	100.986	7.820	8.573	32.386	0.069	3.917	0.002	0.966	0.620
150.749	150.750	15.735	150.749	45.000	-124.163	102.696	37.747	7.672	33.256	0.042	4.494	3.234	0.191	0.070
150.752	150.753	3.031	150.753	45.000	-124.167	104.367	67.969	6.992	33.838	0.046	4.455	1.815	0.192	0.105
150.756	150.757	4.231	150.756	45.000	-124.170	106.102	97.652	6.620	33.927	0.073	4.307	1.578	0.193	0.240
150.759	150.760	25.847	150.760	45.000	-124.173	107.682	18.255	8.392	32.470	0.062	4.076	2.813	0.769	0.470
150.765	150.766	2.545	150.766	45.000	-124.180	111.270	47.993	7.614	33.384	0.043	4.501	2.439	0.190	0.064
150.768	150.770	1.880	150.769	45.000	-124.184	113.287	78.815	6.910	33.863	0.041	4.485	1.496	0.190	0.078
150.772	150.773	6.310	150.773	45.000	-124.188	115.231	106.530	6.668	33.923	0.091	4.202	1.311	0.191	0.339
150.776	150.777	31.676	150.776	45.000	-124.192	117.447	19.457	8.713	32.325	0.071	3.964	2.404	0.891	0.581
150.779	150.780	8.966	150.780	45.000	-124.196	119.441	27.883	8.143	32.491	0.048	4.437	3.068	0.226	0.121
150.782	150.784	2.985	150.783	45.000	-124.200	121.465	57.729	7.600	33.555	0.043	4.485	2.008	0.189	0.078
150.786	150.787	1.322	150.787	45.000	-124.204	123.863	88.047	6.932	33.856	0.040	4.492	1.562	0.189	0.072
150.790	150.791	5.929	150.790	45.000	-124.208	126.065	117.073	6.713	33.921	0.120	4.078	1.388	0.191	0.458

Table C1. (continued)

POC Start time	POC End time	OC [µM]	Insitu Time	Lat	Long	Ship Depth [m]	Fish Depth [m]	T [ºC]	S [PSU]	Backscatter [V]	Transmissometery [V]	O2 [V]	Chlorophyll Fluorescence [v]	Cp [m^{-1}]
150.792	150.793	2.430	150.792	45.000	-124.210	127.435	77.218	7.174	33.784	0.043	4.483	1.664	0.188	0.079
150.795	150.796	28.742	150.796	45.000	-124.214	129.828	12.141	9.366	31.886	0.069	3.975	1.585	0.905	0.563
150.799	150.800	2.506	150.799	45.000	-124.218	132.173	41.311	7.720	33.190	0.046	4.461	2.312	0.194	0.100
150.802	150.803	2.603	150.803	45.000	-124.223	134.362	71.513	7.228	33.782	0.042	4.485	1.677	0.188	0.078
150.806	150.807	4.335	150.806	45.000	-124.226	137.700	102.229	6.908	33.852	0.042	4.482	1.414	0.187	0.080
150.809	150.810	4.149	150.810	45.000	-124.230	138.865	128.832	6.636	33.917	0.083	4.254	1.343	0.187	0.290
150.813	150.814	6.500	150.813	45.000	-124.235	141.010	41.181	7.909	32.944	0.044	4.472	2.386	0.201	0.089
150.816	150.817	16.617	150.817	45.000	-124.239	143.348	25.045	8.913	31.995	0.054	4.340	3.560	0.341	0.210
150.822	150.823	3.186	150.823	45.000	-124.245	146.583	77.056	7.390	33.696	0.044	4.469	1.771	0.187	0.092
150.826	150.827	1.950	150.826	45.000	-124.249	148.297	107.997	6.802	33.880	0.041	4.499	1.445	0.188	0.065
150.829	150.830	4.518	150.830	45.000	-124.252	150.303	138.230	6.596	33.926	0.105	4.136	1.305	0.188	0.403
150.833	150.834	1.829	150.833	45.000	-124.256	151.900	70.966	7.448	33.638	0.041	4.495	1.766	0.187	0.069
150.836	150.838	20.458	150.837	45.000	-124.261	153.856	13.517	9.370	31.814	0.066	4.112	1.811	0.668	0.431
150.840	150.841	4.914	150.840	45.000	-124.265	155.666	43.548	7.546	32.960	0.039	4.496	3.030	0.197	0.068
150.843	150.844	2.876	150.844	45.000	-124.269	157.354	73.302	7.691	33.466	0.037	4.526	2.387	0.187	0.042
150.847	150.848	2.298	150.847	45.000	-124.273	158.443	103.496	7.275	33.757	0.041	4.490	1.705	0.188	0.073
150.860	150.861	14.207	150.860	45.000	-124.288	163.133	20.445	9.344	31.975	0.043	4.301	4.416	0.431	0.248
150.863	150.865	3.494	150.864	45.000	-124.292	163.777	50.272	7.650	33.085	0.035	4.532	3.089	0.188	0.036
150.867	150.868	2.028	150.867	45.000	-124.296	165.102	80.280	7.785	33.626	0.036	4.539	2.162	0.187	0.030
150.870	150.872	1.314	150.871	45.000	-124.300	166.492	110.776	7.307	33.816	0.034	4.546	1.879	0.187	0.023
150.874	150.875	1.787	150.875	45.000	-124.304	167.992	142.035	6.753	33.887	0.041	4.486	1.413	0.186	0.077
150.877	150.879	2.634	150.878	45.000	-124.308	169.417	129.051	7.015	33.845	0.038	4.505	1.597	0.187	0.060
150.881	150.882	3.484	150.882	45.000	-124.313	171.138	36.637	7.811	32.586	0.033	4.503	3.713	0.219	0.062
150.884	150.886	4.767	150.885	45.000	-124.317	173.409	22.411	8.803	32.142	0.035	4.408	4.567	0.328	0.147
150.890	150.891	2.674	150.891	45.000	-124.324	176.213	72.160	7.758	33.499	0.035	4.537	2.616	0.187	0.032
150.894	150.895	1.653	150.894	45.000	-124.328	178.705	102.314	7.493	33.760	0.032	4.548	2.075	0.188	0.022
150.897	150.898	1.962	150.898	45.000	-124.332	180.617	133.032	7.007	33.849	0.038	4.504	1.638	0.188	0.061
150.901	150.902	1.812	150.901	45.000	-124.336	183.494	163.354	6.727	33.916	0.040	4.503	1.454	0.185	0.062
150.904	150.905	2.604	150.905	45.000	-124.340	186.076	127.204	7.183	33.816	0.036	4.523	1.684	0.188	0.044
150.908	150.909	5.631	150.908	45.000	-124.344	189.479	32.008	8.162	32.365	0.041	4.456	4.260	0.281	0.104
150.911	150.912	2.318	150.912	45.000	-124.347	193.074	49.782	7.774	32.799	0.031	4.522	4.205	0.200	0.045
150.915	150.916	2.229	150.915	45.000	-124.351	195.751	140.128	7.150	33.826	0.036	4.523	1.687	0.189	0.044
150.923	150.924	2.279	150.924	45.000	-124.359	203.498	134.685	7.221	33.806	0.034	4.528	1.657	0.188	0.040
150.926	150.928	1.549	150.927	45.000	-124.363	206.885	104.596	7.650	33.663	0.033	4.545	2.157	0.186	0.024
150.930	150.931	1.394	150.931	45.000	-124.366	210.948	74.234	7.892	33.385	0.034	4.541	2.683	0.190	0.029
150.934	150.935	3.396	150.934	45.000	-124.370	215.528	44.023	7.791	32.614	0.034	4.521	4.020	0.209	0.046

Table C1. (continued)

POC Start time	POC End time	OC [µM]	Insitu Time	Lat	Long	Ship Depth [m]	Fish Depth [m]	T [ºC]	S [PSU]	Backscatter [V]	Transmissometery [V]	O2 [V]	Chlorophyll Fluorescence [v]	Cp [m^{-1}]
150.937	150.938	38.755	150.938	45.000	-124.375	219.960	12.753	10.389	31.444	0.064	3.923	2.703	0.908	0.626
150.941	150.942	2.095	150.941	45.000	-124.378	223.190	69.178	7.889	33.163	0.031	4.540	3.155	0.194	0.029
150.944	150.945	1.359	150.945	45.000	-124.382	227.289	157.528	6.933	33.869	0.035	4.520	1.585	0.189	0.046
150.948	150.949	4.099	150.948	45.000	-124.385	231.506	211.679	6.509	33.945	0.055	4.399	1.263	0.187	0.156
150.955	150.957	2.554	150.956	45.000	-124.393	241.184	144.886	7.046	33.854	0.035	4.540	1.670	0.193	0.029
150.959	150.960	1.616	150.959	45.000	-124.397	245.758	114.563	7.654	33.749	0.033	4.553	2.015	0.188	0.018
150.962	150.963	1.956	150.963	45.000	-124.401	250.986	84.635	7.912	33.504	0.032	4.548	2.391	0.189	0.022
150.966	150.967	3.282	150.966	45.000	-124.405	256.918	54.352	8.142	32.759	0.029	4.541	3.470	0.204	0.028
150.969	150.971	7.250	150.970	45.000	-124.409	262.602	23.580	9.953	32.185	0.027	4.460	3.804	0.289	0.100
150.973	150.974	15.323	150.973	45.000	-124.413	269.000	20.831	10.033	31.926	0.039	4.250	2.765	0.456	0.304
150.976	150.977	2.694	150.977	45.000	-124.417	274.201	109.832	7.665	33.681	0.033	4.552	2.236	0.190	0.018
150.980	150.981	2.405	150.980	45.000	-124.421	279.439	200.925	6.621	33.912	0.033	4.544	1.438	0.188	0.025
150.985	150.986	3.145	150.985	45.000	-124.426	286.504	224.226	6.511	33.929	0.034	4.543	1.397	0.189	0.026
150.988	150.989	2.062	150.989	45.000	-124.429	291.003	193.155	6.692	33.904	0.034	4.539	1.495	0.193	0.030
150.992	150.993	1.599	150.992	45.000	-124.432	295.727	163.129	6.966	33.870	0.032	4.549	1.644	0.195	0.021
150.995	150.996	1.664	150.996	45.000	-124.435	300.157	132.708	7.361	33.801	0.031	4.555	2.001	0.189	0.016
150.999	151.000	7.492	150.999	45.000	-124.439	304.950	102.498	7.736	33.628	0.032	4.554	2.410	0.188	0.016
151.002	151.003	1.646	151.003	45.000	-124.443	310.494	72.177	8.138	33.311	0.030	4.555	2.898	0.189	0.016
151.006	151.007	6.129	151.006	45.000	-124.447	316.407	42.055	8.834	32.489	0.028	4.528	3.840	0.240	0.040
151.009	151.011	18.309	151.010	45.000	-124.451	322.343	11.101	11.075	31.634	0.040	4.286	3.092	0.362	0.264
151.020	151.021	1.030	151.020	45.000	-124.463	337.303	251.155	6.358	33.952	0.031	4.558	1.355	0.187	0.013
151.023	151.024	1.562	151.024	45.000	-124.467	342.085	232.692	6.483	33.933	0.031	4.555	1.412	0.190	0.015
151.027	151.028	2.235	151.027	45.000	-124.470	346.205	254.899	6.342	33.954	0.030	4.556	1.350	0.195	0.015
151.030	151.031	2.133	151.031	45.000	-124.474	350.305	256.143	6.334	33.957	0.031	4.546	1.273	0.200	0.024
151.034	151.035	2.233	151.034	45.000	-124.477	353.861	228.074	6.489	33.936	0.028	4.567	1.413	0.203	0.005
151.037	151.038	2.255	151.038	45.000	-124.480	357.392	197.689	6.787	33.886	0.029	4.567	1.681	0.202	0.005
151.041	151.042	0.836	151.041	45.000	-124.484	362.193	167.306	7.072	33.862	0.031	4.557	1.819	0.197	0.014
151.044	151.045	1.594	151.045	45.000	-124.488	367.789	137.147	7.369	33.795	0.031	4.556	2.064	0.193	0.015
151.654	151.655	32.349	151.654	43.920	-124.942	417.688	4.517	10.680	31.853	0.056	3.972	2.733	0.634	0.563
151.657	151.658	23.359	151.658	43.920	-124.941	415.026	23.020	10.397	31.891	0.055	4.031	2.668	0.647	0.506
151.661	151.662	1.993	151.661	43.920	-124.939	406.686	112.350	8.056	33.732	0.032	4.558	1.282	0.166	0.013
151.664	151.665	2.937	151.664	43.920	-124.937	401.217	197.374	6.642	33.949	0.038	4.523	0.919	0.192	0.044
151.668	151.669	4.397	151.668	43.920	-124.934	397.227	290.098	6.293	33.982	0.091	4.302	0.840	0.193	0.244
151.671	151.672	1.847	151.672	43.920	-124.931	378.490	246.919	6.429	33.971	0.060	4.428	0.890	0.190	0.129
151.675	151.676	2.067	151.675	43.920	-124.928	366.898	186.256	6.775	33.923	0.047	4.472	0.972	0.194	0.089
151.678	151.679	7.813	151.679	43.920	-124.925	355.984	126.009	7.642	33.795	0.035	4.540	1.187	0.192	0.029
151.683	151.684	22.100	151.684	43.920	-124.921	334.125	14.339	10.584	31.816	0.052	4.096	3.737	0.550	0.441

Table C1. (continued)

POC Start time	POC End time	OC [µM]	Insitu Time	Lat	Long	Ship Depth [m]	Fish Depth [m]	T [ºC]	S [PSU]	Backscatter [V]	Transmissometery [V]	O2 [V]	Chlorophyll Fluorescence [v]	Cp [m^{-1}]
151.686	151.688	2.270	151.687	43.920	-124.918	318.255	93.284	7.979	33.487	0.036	4.541	1.591	0.194	0.028
151.690	151.691	2.095	151.691	43.920	-124.915	305.823	183.981	6.820	33.912	0.046	4.489	0.997	0.195	0.074
151.694	151.695	3.268	151.694	43.920	-124.913	294.090	276.403	6.207	33.989	0.095	4.283	0.867	0.192	0.262
151.697	151.698	2.577	151.698	43.920	-124.910	285.400	204.081	6.663	33.946	0.040	4.511	0.971	0.197	0.055
151.701	151.702	1.359	151.701	43.920	-124.907	261.659	113.637	7.571	33.670	0.040	4.516	1.239	0.198	0.050
151.704	151.705	15.492	151.705	43.920	-124.904	259.560	23.062	10.156	31.853	0.049	4.241	3.128	0.445	0.305
151.708	151.709	1.679	151.708	43.920	-124.901	251.509	79.646	8.013	33.241	0.034	4.539	2.030	0.198	0.030
151.724	151.725	3.285	151.724	43.920	-124.888	170.720	110.465	7.581	33.650	0.040	4.520	1.463	0.198	0.047
151.727	151.729	1.656	151.728	43.919	-124.885	173.355	146.476	7.067	33.826	0.045	4.481	1.103	0.198	0.081
151.731	151.732	1.417	151.732	43.919	-124.882	172.889	116.470	7.344	33.738	0.043	4.499	1.262	0.200	0.065
151.734	151.736	1.897	151.735	43.920	-124.879	166.391	85.729	7.858	33.429	0.038	4.535	1.753	0.199	0.034
151.738	151.739	2.954	151.739	43.920	-124.876	178.344	55.695	7.965	32.684	0.040	4.518	2.708	0.213	0.049
151.741	151.743	11.579	151.742	43.920	-124.872	193.118	25.005	9.616	31.948	0.055	4.266	3.108	0.461	0.278
151.745	151.746	7.605	151.746	43.920	-124.868	198.647	30.470	9.216	32.088	0.049	4.352	3.322	0.326	0.200
151.748	151.750	2.108	151.749	43.920	-124.865	198.067	120.123	7.219	33.777	0.045	4.489	1.320	0.199	0.074
151.763	151.764	22.111	151.764	43.920	-124.849	191.119	83.629	7.735	33.542	0.037	4.529	1.790	0.199	0.039
151.767	151.768	2.755	151.767	43.920	-124.845	188.501	53.601	7.946	32.628	0.037	4.504	2.954	0.221	0.061
151.770	151.772	36.228	151.771	43.920	-124.841	186.005	22.588	10.028	31.948	0.067	3.834	3.916	1.079	0.707
151.774	151.775	15.827	151.774	43.920	-124.837	183.543	38.647	8.704	32.294	0.050	4.275	3.530	0.508	0.281
151.777	151.778	1.640	151.778	43.920	-124.833	181.170	127.428	6.999	33.849	0.050	4.455	1.202	0.202	0.104
151.781	151.782	2.132	151.781	43.920	-124.830	181.157	156.809	6.748	33.913	0.054	4.437	1.037	0.198	0.121
151.784	151.785	1.586	151.785	43.920	-124.827	182.996	126.610	7.012	33.846	0.050	4.451	1.213	0.202	0.108
151.788	151.789	1.764	151.788	43.920	-124.823	185.793	96.262	7.379	33.713	0.041	4.496	1.390	0.200	0.068
151.799	151.801	32.112	151.800	43.920	-124.811	153.374	20.191	9.334	32.093	0.068	3.957	2.570	0.950	0.600
151.803	151.804	2.041	151.803	43.920	-124.807	147.670	108.736	7.218	33.768	0.047	4.470	1.306	0.202	0.092
151.806	151.808	3.923	151.807	43.920	-124.804	145.372	107.144	6.942	33.865	0.054	4.424	1.164	0.204	0.132
151.810	151.811	2.589	151.810	43.920	-124.800	149.317	77.305	7.660	33.417	0.037	4.522	1.779	0.201	0.045
151.813	151.815	5.598	151.814	43.920	-124.796	144.353	46.490	7.961	32.729	0.043	4.469	2.502	0.231	0.092
151.817	151.818	61.113	151.817	43.920	-124.792	142.366	15.845	9.881	31.978	0.105	3.309	4.222	2.127	1.296
151.820	151.821	2.954	151.821	43.920	-124.789	145.716	55.798	7.825	33.001	0.041	4.502	2.237	0.206	0.062
151.824	151.825	2.254	151.824	43.920	-124.785	149.910	133.714	6.586	33.940	0.073	4.351	1.012	0.204	0.199
151.831	151.833	2.018	151.832	43.920	-124.778	165.402	67.336	7.739	33.155	0.040	4.511	1.991	0.207	0.055
151.835	151.836	9.912	151.836	43.920	-124.775	165.336	37.038	8.230	32.350	0.046	4.412	2.551	0.314	0.145
151.838	151.840	67.039	151.839	43.920	-124.771	167.571	7.057	9.887	31.954	0.095	3.240	0.001	2.282	1.379
151.842	151.843	2.662	151.843	43.920	-124.768	168.574	73.924	7.529	33.502	0.039	4.501	1.895	0.197	0.064
151.845	151.847	2.218	151.846	43.920	-124.765	169.728	158.597	6.535	33.950	0.083	4.305	0.996	0.204	0.241
151.849	151.850	2.161	151.850	43.919	-124.762	171.406	130.530	6.706	33.909	0.064	4.373	0.993	0.204	0.179

Table C1. (continued)

POC Start time	POC End time	OC [µM]	Insitu Time	Lat	Long	Ship Depth [m]	Fish Depth [m]	T [ºC]	S [PSU]	Backscatter [V]	Transmissometery [V]	O2 [V]	Chlorophyll Fluorescence [v]	Cp [m^{-1}]
151.988	151.989	3.113	151.988	43.920	-124.627	209.613	161.149	6.692	33.948	0.103	4.187	0.916	0.208	0.353
151.991	151.993	0.689	151.992	43.920	-124.624	209.595	131.060	6.945	33.929	0.032	4.552	1.108	0.204	0.019
152.001	152.002	2.149	152.001	43.920	-124.615	207.563	49.504	7.714	33.317	0.036	4.529	1.655	0.203	0.039
152.004	152.006	27.221	152.005	43.920	-124.612	206.907	18.947	8.394	32.527	0.063	4.164	3.216	0.680	0.398
152.008	152.009	6.632	152.008	43.920	-124.608	205.920	47.592	7.688	33.303	0.036	4.526	2.184	0.205	0.041
152.011	152.012	1.482	152.012	43.920	-124.605	203.750	136.964	6.936	33.930	0.038	4.522	1.159	0.200	0.045
152.015	152.016	2.875	152.015	43.920	-124.602	202.669	181.192	6.670	33.950	0.116	4.129	0.927	0.205	0.409
152.018	152.019	1.807	152.019	43.920	-124.599	201.086	150.604	6.793	33.939	0.067	4.348	0.980	0.204	0.202
152.022	152.023	0.879	152.022	43.920	-124.596	199.513	120.306	7.081	33.918	0.032	4.553	1.146	0.202	0.018
152.025	152.027	6.597	152.026	43.920	-124.593	197.809	89.396	7.273	33.821	0.040	4.496	1.144	0.204	0.068
152.038	152.039	2.822	152.038	43.920	-124.580	189.788	62.695	7.561	33.610	0.038	4.514	1.585	0.204	0.052
152.041	152.043	4.766	152.042	43.920	-124.577	187.291	154.095	6.750	33.943	0.098	4.229	0.986	0.204	0.314
152.045	152.046	4.463	152.046	43.920	-124.573	184.237	156.603	6.729	33.944	0.110	4.169	0.955	0.204	0.370
152.048	152.050	0.824	152.049	43.920	-124.570	181.806	126.922	6.987	33.925	0.038	4.526	1.093	0.201	0.041
152.052	152.053	0.809	152.053	43.920	-124.567	179.045	96.387	7.314	33.891	0.032	4.547	1.190	0.201	0.023
152.056	152.057	2.109	152.056	43.920	-124.564	175.458	66.398	7.472	33.686	0.036	4.506	1.218	0.204	0.059
152.059	152.060	2.531	152.060	43.920	-124.561	171.822	36.258	7.737	33.097	0.034	4.533	2.012	0.204	0.035
152.091	152.092	3.433	152.091	43.920	-124.535	144.028	117.916	7.051	33.920	0.056	4.416	1.069	0.203	0.141
152.066	152.067	3.630	152.067	43.920	-124.555	163.207	70.192	7.442	33.720	0.037	4.508	1.361	0.199	0.057
152.070	152.071	4.687	152.070	43.920	-124.552	158.936	147.413	6.847	33.936	0.117	4.145	0.942	0.205	0.393
152.073	152.074	1.294	152.074	43.920	-124.549	155.270	116.965	7.041	33.920	0.041	4.504	1.064	0.200	0.061
152.077	152.078	1.163	152.077	43.920	-124.546	151.287	86.696	7.397	33.879	0.035	4.538	1.236	0.200	0.031
152.080	152.081	2.056	152.081	43.920	-124.543	148.324	56.579	7.651	33.526	0.037	4.525	1.468	0.204	0.042
152.084	152.085	12.126	152.084	43.920	-124.540	146.111	26.412	7.832	32.832	0.040	4.475	2.608	0.255	0.087
152.087	152.088	7.737	152.088	43.920	-124.538	144.871	26.561	8.036	32.870	0.049	4.298	3.069	0.525	0.263
152.098	152.099	2.147	152.098	43.920	-124.530	142.957	80.347	7.481	33.864	0.032	4.543	1.184	0.200	0.026
152.101	152.103	3.471	152.102	43.920	-124.528	142.690	49.935	7.706	33.449	0.034	4.528	1.469	0.204	0.040
152.105	152.106	31.444	152.105	43.920	-124.526	142.326	19.748	8.257	32.685	0.064	4.092	2.747	0.726	0.456
152.108	152.109	5.591	152.109	43.920	-124.524	141.860	46.309	7.725	33.343	0.035	4.529	1.944	0.203	0.039
152.112	152.113	3.939	152.112	43.920	-124.521	141.344	129.840	6.990	33.925	0.078	4.310	0.991	0.207	0.237
152.115	152.117	1.068	152.116	43.920	-124.519	140.758	100.973	7.244	33.897	0.034	4.536	1.132	0.200	0.032
152.119	152.120	3.467	152.119	43.920	-124.517	140.186	70.851	7.430	33.753	0.039	4.511	1.159	0.204	0.054
152.122	152.124	6.302	152.123	43.920	-124.515	139.583	40.498	7.749	33.237	0.036	4.529	1.679	0.208	0.039
152.126	152.127	74.610	152.126	43.920	-124.513	139.006	9.957	9.420	32.482	0.116	3.222	2.375	2.344	1.414
152.129	152.130	2.136	152.130	43.920	-124.511	138.286	74.081	7.496	33.788	0.034	4.529	1.284	0.203	0.039
152.133	152.134	2.437	152.133	43.920	-124.509	137.590	115.194	7.068	33.917	0.043	4.482	1.054	0.203	0.080
152.136	152.137	2.171	152.137	43.920	-124.507	136.780	84.818	7.386	33.879	0.033	4.537	1.165	0.202	0.032

Table C1. (continued)

POC Start time	POC End time	OC [µM]	Insitu Time	Lat	Long	Ship Depth [m]	Fish Depth [m]	T [ºC]	S [PSU]	Backscatter [V]	Transmissometery [V]	O2 [V]	Chlorophyll Fluorescence [v]	Cp [m^{-1}]
152.140	152.141	2.793	152.140	43.920	-124.505	135.817	54.610	7.632	33.580	0.035	4.523	1.335	0.210	0.044
152.143	152.145	4.587	152.144	43.920	-124.502	134.910	24.046	7.896	32.631	0.036	4.501	2.478	0.228	0.063
152.147	152.148	3.535	152.147	43.920	-124.500	134.235	33.606	7.794	32.964	0.033	4.520	2.728	0.206	0.046
152.150	152.152	2.300	152.151	43.920	-124.498	133.531	120.739	7.031	33.921	0.045	4.470	1.111	0.205	0.092
152.156	152.157	1.402	152.156	43.920	-124.496	132.623	78.783	7.462	33.866	0.035	4.539	1.167	0.203	0.030
152.159	152.161	23.114	152.160	43.920	-124.494	132.088	47.046	7.761	33.358	0.035	4.526	1.547	0.208	0.042
152.163	152.164	9.820	152.163	43.920	-124.492	131.628	18.047	8.132	32.518	0.049	4.373	2.879	0.358	0.181
152.166	152.168	1.853	152.167	43.920	-124.490	131.203	55.319	7.679	33.500	0.035	4.524	1.532	0.205	0.043
152.170	152.171	2.826	152.170	43.920	-124.488	130.863	113.871	7.069	33.917	0.040	4.504	1.060	0.205	0.061
152.173	152.175	5.291	152.174	43.920	-124.486	130.549	83.502	7.365	33.871	0.033	4.537	1.202	0.203	0.032
152.177	152.178	5.040	152.178	43.920	-124.485	130.283	53.204	7.720	33.500	0.034	4.524	1.428	0.208	0.043
152.180	152.182	5.647	152.181	43.920	-124.483	129.990	23.148	7.814	32.741	0.033	4.524	2.546	0.216	0.043
152.184	152.186	2.897	152.185	43.920	-124.480	129.759	47.316	7.722	33.345	0.035	4.526	1.940	0.201	0.041
152.188	152.189	2.983	152.188	43.920	-124.479	129.407	115.944	6.977	33.926	0.067	4.368	1.038	0.209	0.185
152.191	152.193	3.142	152.192	43.920	-124.477	129.120	85.250	7.401	33.868	0.035	4.539	1.176	0.204	0.030
152.195	152.196	2.665	152.195	43.920	-124.475	128.773	55.063	7.704	33.485	0.036	4.517	1.438	0.209	0.049
152.198	152.200	5.213	152.199	43.920	-124.473	128.442	24.542	7.819	32.733	0.033	4.523	2.661	0.217	0.044
152.202	152.203	4.092	152.202	43.920	-124.471	127.946	32.094	7.819	32.954	0.035	4.495	2.784	0.242	0.071
152.205	152.207	2.948	152.206	43.920	-124.469	127.643	114.237	6.945	33.930	0.085	4.282	0.997	0.211	0.264
152.209	152.210	5.252	152.209	43.920	-124.467	127.318	87.118	7.301	33.874	0.032	4.542	1.110	0.206	0.027
152.214	152.215	6.133	152.215	43.920	-124.465	126.867	40.828	7.766	33.229	0.034	4.522	1.758	0.212	0.045
152.218	152.219	68.868	152.218	43.920	-124.463	126.637	9.864	9.261	32.400	0.103	3.419	2.518	1.806	1.212
152.221	152.222	3.960	152.222	43.920	-124.461	126.486	74.011	7.489	33.813	0.035	4.536	1.342	0.208	0.033
152.225	152.226	4.147	152.225	43.919	-124.459	126.545	99.847	7.083	33.916	0.036	4.532	1.077	0.207	0.036
152.228	152.229	3.124	152.229	43.919	-124.457	126.581	69.595	7.586	33.802	0.037	4.534	1.197	0.209	0.034
152.232	152.233	4.148	152.232	43.919	-124.456	126.805	39.337	7.830	33.166	0.036	4.519	1.943	0.215	0.047
152.235	152.237	79.946	152.236	43.919	-124.454	126.430	8.100	9.620	32.310	0.099	3.373	1.843	1.856	1.243
152.239	152.240	1.676	152.239	43.919	-124.452	124.173	80.197	7.362	33.849	0.034	4.538	1.166	0.208	0.031
152.252	152.253	35.402	152.252	43.920	-124.446	119.910	12.248	8.719	32.401	0.080	4.025	3.130	0.928	0.549
152.255	152.256	3.235	152.256	43.920	-124.444	119.464	67.931	7.469	33.750	0.038	4.521	1.245	0.209	0.046
152.259	152.260	5.557	152.259	43.920	-124.442	118.422	93.698	7.160	33.910	0.033	4.545	1.111	0.208	0.025
152.262	152.263	4.208	152.263	43.920	-124.440	118.032	63.782	7.507	33.700	0.038	4.517	1.224	0.210	0.049
152.266	152.267	4.105	152.266	43.920	-124.439	116.257	33.568	8.015	33.138	0.040	4.484	1.890	0.231	0.079
152.269	152.271	80.422	152.270	43.920	-124.437	116.519	11.672	9.041	32.526	0.075	3.745	1.663	1.395	0.858
152.273	152.274	4.302	152.273	43.920	-124.435	122.757	95.560	7.129	33.910	0.045	4.477	0.970	0.210	0.085
152.276	152.277	7.281	152.277	43.920	-124.433	120.799	87.550	7.187	33.906	0.034	4.543	2.094	0.209	0.026
152.283	152.284	5.361	152.283	43.920	-124.430	120.049	31.997	8.119	33.124	0.040	4.459	2.541	0.248	0.101

Table C1. (continued)

POC Start time	POC End time	OC [µM]	Insitu Time	Lat	Long	Ship Depth [m]	Fish Depth [m]	T [ºC]	S [PSU]	Backscatter [V]	Transmissometery [V]	O2 [V]	Chlorophyll Fluorescence [v]	Cp [m^{-1}]
152.286	152.288	46.702	152.287	43.920	-124.428	119.390	14.601	8.838	32.653	0.079	3.781	1.332	1.294	0.825
152.290	152.291	7.493	152.290	43.920	-124.426	119.199	98.315	7.125	33.912	0.051	4.467	1.022	0.211	0.095
152.293	152.294	3.282	152.293	43.920	-124.424	119.030	85.470	7.267	33.897	0.032	4.547	1.072	0.210	0.022
152.296	152.298	6.387	152.297	43.920	-124.422	118.879	55.444	7.654	33.616	0.028	4.521	4.206	0.213	0.046
152.300	152.301	9.575	152.300	43.920	-124.420	118.698	24.946	8.104	32.921	0.031	4.465	3.916	0.260	0.096
152.303	152.304	13.030	152.304	43.920	-124.418	118.380	30.276	8.266	33.056	0.047	4.329	0.603	0.432	0.230
152.307	152.308	10.153	152.308	43.920	-124.416	118.232	106.403	7.045	33.919	0.086	4.276	3.040	0.217	0.272
152.313	152.314	5.821	152.314	43.920	-124.412	118.298	52.895	7.688	33.589	0.032	4.516	3.601	0.215	0.050
152.317	152.318	42.908	152.317	43.920	-124.410	118.341	21.104	8.378	32.822	0.055	4.153	1.603	0.679	0.418
152.320	152.321	8.759	152.321	43.920	-124.408	118.375	37.974	8.012	33.311	0.035	4.436	2.705	0.269	0.123
152.324	152.325	1.664	152.324	43.920	-124.406	118.352	102.547	7.092	33.912	0.070	4.343	3.252	0.215	0.208
152.327	152.328	4.080	152.328	43.920	-124.404	118.249	72.150	7.477	33.807	0.025	4.521	4.785	0.212	0.046
152.331	152.332	16.052	152.331	43.920	-124.402	118.075	41.798	7.966	33.393	0.041	4.454	0.002	0.248	0.106
152.334	152.335	111.779	152.335	43.920	-124.400	117.962	11.757	9.757	32.805	0.129	2.858	0.001	2.776	1.895
152.338	152.339	4.653	152.338	43.920	-124.399	117.939	69.092	7.429	33.793	0.031	4.510	3.353	0.210	0.056
152.347	152.348	10.247	152.347	43.920	-124.394	117.903	45.141	7.815	33.473	0.038	4.489	0.002	0.229	0.075
152.350	152.351	33.410	152.351	43.920	-124.392	117.855	14.997	8.879	32.839	0.086	3.698	0.002	1.288	0.907
152.354	152.355	5.089	152.354	43.920	-124.390	117.906	57.880	7.562	33.688	0.037	4.513	0.106	0.208	0.053
152.357	152.358	2.133	152.358	43.920	-124.389	117.735	95.926	7.137	33.903	0.060	4.369	4.664	0.215	0.182
152.361	152.362	8.102	152.361	43.920	-124.387	117.674	66.606	7.520	33.752	0.036	4.515	0.196	0.213	0.051
152.364	152.365	5.073	152.365	43.920	-124.385	117.638	36.290	7.924	33.336	0.038	4.485	0.002	0.238	0.078
152.368	152.369	87.547	152.368	43.920	-124.383	117.562	7.965	9.633	32.833	0.123	3.014	0.001	2.452	1.711
152.371	152.372	7.204	152.372	43.920	-124.381	117.633	86.337	7.196	33.889	0.041	4.458	4.815	0.211	0.103
152.377	152.378	12.877	152.377	43.920	-124.378	117.640	66.676	7.497	33.741	0.036	4.512	0.326	0.214	0.054
152.380	152.381	4.821	152.381	43.920	-124.376	117.410	37.400	7.933	33.324	0.038	4.485	0.002	0.235	0.078
152.384	152.385	74.969	152.384	43.920	-124.374	117.399	7.571	9.564	32.824	0.124	2.976	0.001	2.519	1.741
152.387	152.388	3.286	152.388	43.920	-124.372	117.339	83.132	7.194	33.887	0.043	4.480	2.503	0.210	0.083
152.391	152.392	5.574	152.391	43.920	-124.370	117.314	86.467	7.124	33.905	0.038	4.518	0.002	0.210	0.049
152.394	152.395	5.785	152.395	43.920	-124.368	116.984	56.293	7.611	33.640	0.035	4.517	0.002	0.215	0.050
152.398	152.399	20.637	152.398	43.920	-124.366	117.083	26.036	8.401	33.218	0.059	4.171	0.002	0.567	0.369
152.401	152.402	14.821	152.402	43.920	-124.364	116.898	28.955	8.260	33.200	0.054	4.217	0.002	0.573	0.341
152.418	152.419		152.419	43.920	-124.355	116.875	45.252	7.784	33.500	0.038	4.486	0.002	0.247	0.077
152.421	152.422	2.285	152.422	43.920	-124.353	116.679	99.066	6.944	33.927	0.032	4.543	0.815	0.210	0.026
152.425	152.426	8.223	152.425	43.920	-124.351	116.658	68.656	7.418	33.783	0.035	4.516	0.046	0.211	0.050
152.428	152.429	9.147	152.429	43.920	-124.349	116.885	38.802	7.910	33.374	0.037	4.483	0.002	0.246	0.080
152.432	152.433	115.734	152.433	43.920	-124.347	116.048	7.789	9.747	32.925	0.143	2.561	0.001	3.727	2.330
152.435	152.436	4.565	152.436	43.920	-124.345	115.800	79.024	7.292	33.846	0.032	4.524	0.715	0.208	0.043

Table C1. (continued)

POC Start time	POC End time	OC [µM]	Insitu Time	Lat	Long	Ship Depth [m]	Fish Depth [m]	T [ºC]	S [PSU]	Backscatter [V]	Transmissometery [V]	O2 [V]	Chlorophyll Fluorescence [v]	Cp [m^{-1}]
152.439	152.440	8.950	152.440	43.920	-124.342	115.526	82.290	7.254	33.884	0.034	4.530	0.043	0.210	0.037
152.442	152.444	31.067	152.443	43.920	-124.340	115.283	52.061	7.645	33.621	0.033	4.524	0.002	0.213	0.043
152.448	152.450	93.102	152.449	43.920	-124.337	114.672	15.945	9.322	33.103	0.117	3.090	0.002	2.697	1.701
152.452	152.453	3.995	152.453	43.920	-124.334	114.444	100.826	6.893	33.932	0.045	4.424	4.735	0.211	0.136
152.455	152.457	4.460	152.456	43.920	-124.332	113.951	75.208	7.358	33.842	0.032	4.530	0.579	0.210	0.038
152.459	152.460	2.720	152.460	43.920	-124.331	113.837	45.551	7.699	33.573	0.032	4.527	0.002	0.214	0.041
152.462	152.464	85.263	152.463	43.920	-124.329	113.606	15.044	9.261	33.168	0.135	2.916	0.001	2.746	1.837
152.466	152.467	5.575	152.467	43.920	-124.327	112.995	60.037	7.522	33.709	0.033	4.521	0.334	0.209	0.045
152.469	152.471	2.533	152.470	43.920	-124.325	112.493	87.963	7.088	33.914	0.030	4.546	0.930	0.211	0.024
152.473	152.474	5.283	152.473	43.920	-124.323	112.321	58.246	7.492	33.734	0.033	4.518	0.002	0.213	0.048
152.477	152.479	45.863	152.478	43.920	-124.321	111.682	19.892	8.689	33.237	0.091	3.614	0.002	1.394	0.965
152.481	152.482	3.662	152.481	43.920	-124.319	111.446	44.421	7.669	33.572	0.033	4.521	0.077	0.205	0.045
152.484	152.485	2.657	152.485	43.920	-124.317	111.186	90.595	6.929	33.921	0.037	4.474	3.863	0.212	0.087
152.488	152.489	2.647	152.488	43.920	-124.316	110.615	60.897	7.478	33.764	0.032	4.524	0.002	0.210	0.044
152.491	152.493	22.999	152.492	43.920	-124.314	110.515	29.633	7.978	33.309	0.039	4.433	0.002	0.296	0.125
152.495	152.496	95.723	152.495	43.920	-124.312	109.764	16.817	8.936	33.227	0.106	3.354	0.002	2.190	1.399
152.498	152.499	6.809	152.499	43.920	-124.310	109.475	97.472	6.749	33.935	0.142	3.982	4.036	0.223	0.554
152.502	152.503	11.696	152.502	43.920	-124.308	108.934	68.347	7.333	33.820	0.036	4.490	1.056	0.213	0.074
152.511	152.512	4.139	152.512	43.920	-124.301	106.822	47.950	7.620	33.612	0.035	4.516	0.002	0.213	0.050
152.515	152.516	5.866	152.515	43.920	-124.299	105.867	84.235	6.856	33.924	0.132	4.057	4.474	0.221	0.479
152.518	152.519	3.767	152.519	43.920	-124.296	105.257	54.893	7.493	33.733	0.035	4.515	0.002	0.213	0.052
152.522	152.523	9.221	152.522	43.920	-124.293	104.095	24.445	7.967	33.267	0.040	4.420	0.002	0.321	0.138
152.525	152.526	10.357	152.526	43.920	-124.290	102.970	33.033	7.831	33.434	0.040	4.436	0.002	0.321	0.126
152.529	152.530	11.224	152.529	43.920	-124.287	101.954	82.701	6.910	33.922	0.103	4.177	4.672	0.217	0.364
152.532	152.533	5.255	152.533	43.920	-124.285	100.708	53.435	7.393	33.758	0.038	4.498	0.002	0.214	0.066
152.536	152.537	17.872	152.536	43.920	-124.281	99.163	22.704	7.968	33.234	0.038	4.464	0.002	0.263	0.097
152.543	152.544	7.626	152.544	43.920	-124.275	95.431	71.089	7.068	33.876	0.055	4.379	4.870	0.215	0.174
152.547	152.548	3.152	152.547	43.920	-124.272	93.727	41.753	7.613	33.651	0.034	4.526	0.002	0.213	0.041
152.550	152.551	59.236	152.551	43.920	-124.269	91.945	10.768	8.856	33.170	0.094	3.479	0.002	1.900	1.190
152.554	152.555	9.077	152.554	43.920	-124.265	90.193	73.606	7.078	33.880	0.091	4.224	3.872	0.218	0.320
152.557	152.559	12.202	152.558	43.920	-124.262	88.512	56.041	7.316	33.790	0.041	4.465	1.338	0.214	0.096
152.561	152.562	4.800	152.561	43.920	-124.259	86.861	26.698	7.821	33.407	0.032	4.525	0.002	0.217	0.042
152.564	152.566	16.393	152.565	43.920	-124.256	85.431	29.139	7.938	33.431	0.040	4.417	0.002	0.363	0.147
152.568	152.569	5.839	152.568	43.920	-124.253	83.933	65.167	7.079	33.883	0.076	4.277	4.500	0.219	0.269
152.576	152.577	11.528	152.577	43.920	-124.246	80.328	40.715	7.616	33.636	0.035	4.504	0.052	0.216	0.061
152.580	152.581	3.678	152.580	43.920	-124.243	78.832	54.065	7.383	33.764	0.042	4.456	1.163	0.215	0.104
152.583	152.584	10.618	152.584	43.920	-124.240	77.129	23.052	7.944	33.322	0.035	4.514	0.002	0.225	0.052

Table C1. (continued)

POC Start time	POC End time	OC [µM]	Insitu Time	Lat	Long	Ship Depth [m]	Fish Depth [m]	T [ºC]	S [PSU]	Backscatter [V]	Transmissometery [V]	O2 [V]	Chlorophyll Fluorescence [v]	Cp [m^{-1}]
152.579	152.588	8.046	152.584	43.920	-124.240	77.342	31.238	7.896	33.445	0.041	4.401	0.317	0.389	0.168
152.590	152.591	8.976	152.591	43.920	-124.235	74.298	48.244	7.436	33.744	0.045	4.450	0.354	0.218	0.109
152.594	152.595	8.695	152.594	43.920	-124.232	72.414	17.549	8.056	33.142	0.037	4.477	0.002	0.256	0.085
152.597	152.598	10.573	152.598	43.920	-124.229	70.368	53.294	7.303	33.803	0.071	4.336	2.603	0.218	0.214
152.601	152.602	9.729	152.601	43.920	-124.226	68.999	37.359	7.679	33.641	0.040	4.484	0.002	0.222	0.079
152.604	152.605	53.294	152.605	43.920	-124.223	65.963	7.485	9.079	33.068	0.074	3.738	0.002	1.582	0.883
152.608	152.609	6.693	152.608	43.920	-124.220	63.728	54.114	7.242	33.831	0.071	4.311	4.870	0.222	0.236
152.611	152.612	3.969	152.612	43.920	-124.217	61.642	23.235	7.954	33.355	0.035	4.503	0.002	0.229	0.062
152.615	152.616	5.683	152.615	43.920	-124.214	59.683	36.073	7.660	33.624	0.045	4.442	0.053	0.242	0.116
152.618	152.619	7.463	152.619	43.919	-124.211	57.791	28.723	7.919	33.491	0.039	4.432	0.002	0.301	0.125
152.622	152.623	64.362	152.622	43.918	-124.208	56.462	8.953	8.996	33.078	0.078	3.545	0.002	2.124	1.139
152.625	152.626	9.645	152.626	43.918	-124.206	54.110	33.602	7.819	33.619	0.045	4.376	0.002	0.327	0.176
152.629	152.630	81.504	152.629	43.918	-124.203	53.156	10.714	8.988	33.142	0.099	3.328	0.002	2.537	1.429

Table C2. - Raw TSS and $\delta^{13}C$ data from W0905B transects at 45ºN and 43.9ºN. Relevant in situ measurements are included. The solid line on page 71 indicates the transition from 45ºN to 43.9ºN data.

TSS Start time	TSS End time	SuperSucker TSS [mg/L]	SuperSucker $\delta^{13}C$	Surface TSS [mg/L]	Surface $\delta^{13}C$	Insitu Time	Lat	Long	Ship Depth [m]	Fish Depth [m]	Suface Depth [m]	T [ºC]	S [PSU]	Backscatter [V]	Xmiss [V]	O_2 [V]	Chl Fluor [V]	Cp [m^{-1}]
150.658	150.661	8.2	-21.0	8.8	-21.1	150.659	45.008	-124.067	49.34	4.90	5	8.477	32.932	0.088	3.782	3.318	0.983	0.771
150.695	150.699	3.4	-21.2	7.6	-20.0	150.697	45.003	-124.109	75.65	34.07	5	7.472	33.360	0.062	4.262	1.818	0.406	0.292
150.730	150.734	2.4	-24.2	2.6	-20.2	150.732	45.000	-124.146	95.21	80.38	5	6.649	33.910	0.066	4.340	1.526	0.196	0.212
150.767	150.771	8.6		6.6		150.769	45.000	-124.184	113.33	79.09	5	6.955	33.850	0.044	4.472	1.504	0.190	0.091
150.812	150.816	2.4	-21.0	2.7	-20.3	150.814	45.000	-124.235	141.52	31.19	5	8.731	32.442	0.057	4.212	2.225	0.551	0.342
150.838	150.842	1.3	-21.9	3.0	-20.4	150.840	45.000	-124.265	155.70	42.86	5	7.667	32.898	0.042	4.486	3.123	0.203	0.077
150.892	150.897	2.3	-24.3	7.2	-20.7	150.894	45.000	-124.328	178.70	104.33	5	7.447	33.763	0.034	4.542	2.016	0.188	0.027
150.925	150.928	3.0		6.6		150.926	45.000	-124.362	206.25	110.35	5	7.592	33.701	0.033	4.548	2.094	0.187	0.023
150.948	150.951	4.8	-24.5	4.4	-20.3	150.950	45.000	-124.386	233.38	198.89	5	6.586	33.927	0.040	4.499	1.470	0.188	0.066
150.974	150.978	3.3		5.3		150.976	45.000	-124.416	272.43	79.53	5	8.101	33.199	0.029	4.538	3.108	0.207	0.031
151.007	151.010	5.6	-22.3	4.4	-21.4	151.008	45.000	-124.449	319.70	24.80	5	9.663	32.373	0.026	4.489	3.842	0.280	0.075
151.656	151.659	3.4	-21.5	2.6	-22.3	151.658	43.920	-124.941	414.75	24.17	5	10.056	32.011	0.051	4.111	2.644	0.556	0.437
151.684	151.688	1.5	-23.0	4.8	-22.4	151.686	43.920	-124.919	322.55	67.42	5	8.516	32.876	0.041	4.459	2.369	0.270	0.105
151.724	151.727	3.3		4.0		151.726	43.920	-124.887	171.85	138.86	5	7.203	33.781	0.044	4.492	1.212	0.198	0.072
151.765	151.767	1.9	-23.0	2.3	-22.6	151.766	43.920	-124.847	189.46	65.14	5	7.869	33.018	0.036	4.526	2.477	0.206	0.041
151.800	151.803	2.8	-23.2	2.9	-20.5	151.801	43.920	-124.809	149.86	57.97	5	7.951	32.966	0.042	4.477	2.540	0.244	0.087
151.833	151.835	2.9		2.9		151.834	43.920	-124.777	165.13	53.66	5	7.851	32.955	0.039	4.491	2.164	0.216	0.073
151.857	151.859	2.6	-23.3	3.7	-19.4	151.858	43.920	-124.755	173.00	58.25	5	7.744	33.179	0.040	4.508	1.969	0.206	0.058
151.892	151.895	4.4	-24.3	5.6	-19.5	151.894	43.920	-124.720	188.55	92.62	5	7.245	33.750	0.039	4.512	1.414	0.201	0.054
151.937	151.940	3.1		3.3		151.938	43.920	-124.674	205.21	77.00	5	7.525	33.642	0.038	4.512	1.405	0.205	0.054
151.968	151.969	4.0	-22.6	8.2	-20.3	151.969	43.920	-124.644	211.75	71.00	5	7.516	33.676	0.037	4.511	1.362	0.204	0.055
152.012	152.015	3.0	-23.5	7.3	-18.5	152.013	43.920	-124.604	203.40	170.77	5	6.727	33.946	0.099	4.226	0.978	0.203	0.323
152.066	152.069	4.0		6.5		152.068	43.920	-124.554	162.05	95.29	5	7.254	33.826	0.046	4.476	1.277	0.200	0.089
152.092	152.096	3.4	-23.8	7.6	-18.8	152.094	43.920	-124.533	143.50	117.79	5	7.062	33.918	0.059	4.410	1.059	0.202	0.149
152.128	152.131	3.2	-23.5	4.5	-17.7	152.129	43.920	-124.511	138.47	54.37	5	7.648	33.412	0.034	4.521	1.984	0.209	0.047
152.166	152.169	4.1	-23.1	8.1	-18.4	152.167	43.920	-124.490	131.15	66.07	5	7.549	33.599	0.035	4.530	1.515	0.204	0.038
152.203	152.205	4.0	-23.9	8.0	-18.6	152.204	43.920	-124.470	127.83	67.91	5	7.525	33.677	0.035	4.524	1.381	0.203	0.044
152.238	152.242	3.4		6.8		152.240	43.919	-124.452	123.54	92.06	5	7.208	33.855	0.051	4.448	1.108	0.210	0.114

Table C2. (continued)

TSS Start time	TSS End time	SuperSucker TSS [mg/L]	SuperSucker $\delta^{13}C$	Surface TSS [mg/L]	Surface $\delta^{13}C$	Insitu Time	Lat	Long	Ship Depth [m]	Fish Depth [m]	Suface Depth [m]	T [ºC]	S [PSU]	Backscatter [V]	Xmiss [V]	O_2 [V]	Chl Fluor [v]	Cp [m^{-1}]
152.270	152.273	4.0	-21.5	5.9	-18.3	152.271	43.920	-124.436	119.70	47.69	5	7.758	33.352	0.037	4.492	1.827	0.236	0.074
152.303	152.305	4.3	-22.5	5.9	-18.1	152.304	43.920	-124.418	118.38	33.85	5	8.422	33.152	0.058	4.119	1.260	0.807	0.489
152.354	152.356	3.0	-22.8	4.2	-18.2	152.355	43.920	-124.390	117.82	82.03	5	7.253	33.835	0.059	4.387	3.073	0.212	0.173
152.388	152.392	5.0	-23.7	10.7	-17.4	152.390	43.920	-124.370	117.26	93.07	5	7.010	33.917	0.074	4.314	2.740	0.212	0.242
152.408	152.411	2.8	-24.1	7.8	-17.8	152.409	43.920	-124.360	116.96	71.21	5	7.397	33.788	0.036	4.505	0.068	0.212	0.065
152.437	152.440	3.3	-23.7	10.4	-17.8	152.439	43.920	-124.343	115.73	88.08	5	7.152	33.900	0.032	4.536	0.827	0.210	0.033
152.454	152.458	2.6	-23.1	7.1	-17.8	152.456	43.920	-124.333	113.97	77.16	5	7.318	33.843	0.030	4.525	2.009	0.210	0.043
152.485	152.490	2.5		17.1		152.487	43.920	-124.316	110.79	68.44	5	7.337	33.819	0.033	4.523	0.812	0.211	0.044
152.514	152.516	2.6	-22.7	16.7	-17.7	152.515	43.920	-124.299	106.04	87.54	5	6.850	33.924	0.139	4.026	4.373	0.222	0.517
152.554	152.557	3.1	-22.1	8.6	-17.7	152.555	43.920	-124.264	89.65	74.45	5	7.025	33.899	0.104	4.169	4.378	0.219	0.376
152.578	152.581	3.3	-19.8	12.1	-17.8	152.580	43.920	-124.244	79.03	57.84	5	7.288	33.803	0.058	4.387	2.511	0.218	0.170
152.613	152.614	8.0		9.2		152.614	43.920	-124.215	60.92	8.28	5	9.048	33.052	0.082	3.620	0.002	1.802	1.029

Appendix D

Figure D1. – Separation of water column into three particle pools, with b_b:c_p overlaid in color..

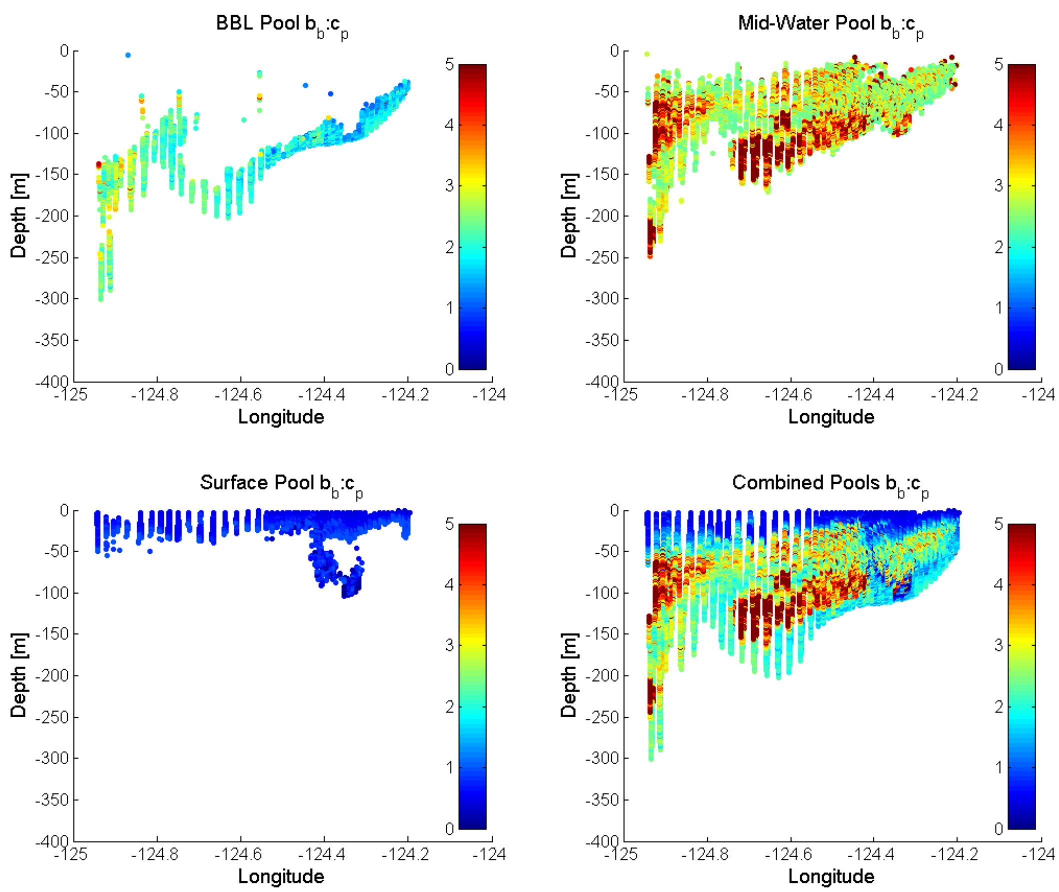

Figure D2. – Separation of water column into three particle pools, with b_b:c_p overlaid in color.

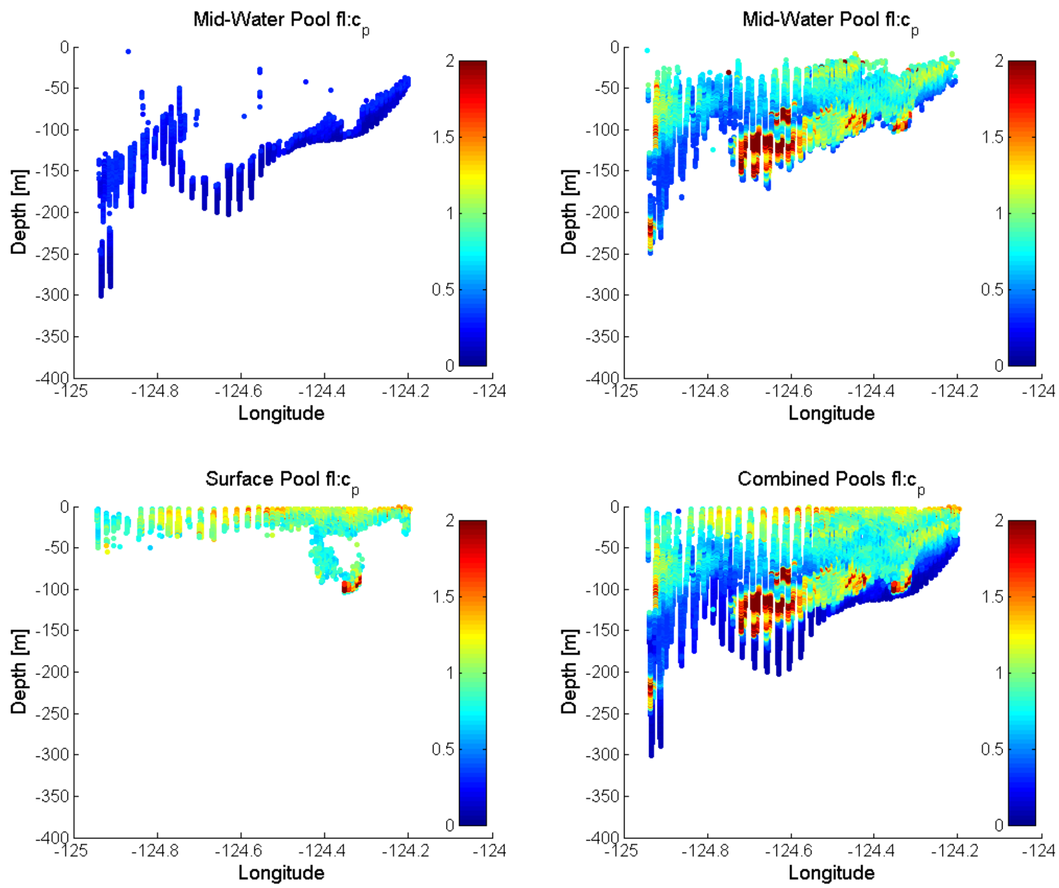

Figure D3. – Separation of water column into three particle pools, with reconstructed POC [μM] overlaid in color.